

Fahlore Thermochemistry: Gaps Inside the $(\text{Cu,Ag})_{10}(\text{Fe,Zn})_2(\text{Sb,As})_4\text{S}_{13}$ Cube¹

R. O. Sack

OFM Research Corporation, Redmond, WA, USA

e-mail: fahlore@century.net

Received December 10, 2016; in final form, March 21, 2017

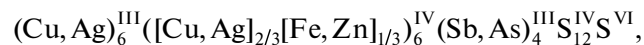
Abstract—Possible topologies of miscibility gaps in arsenian $(\text{Cu,Ag})_{10}(\text{Fe,Zn})_2(\text{Sb,As})_4\text{S}_{13}$ fahlores are examined. These topologies are based on a thermodynamic model for fahlores whose calibration has been verified for $(\text{Cu,Ag})_{10}(\text{Fe,Zn})_2\text{Sb}_4\text{S}_{13}$ fahlores, and conform with experimental constraints on the incompatibility between As and Ag in $(\text{Cu,Ag})_{10}(\text{Fe,Zn})_2(\text{Sb,As})_4\text{S}_{13}$ fahlores, and with experimental and natural constraints on the incompatibility between As and Zn and the nonideality of the As for Sb substitution in $\text{Cu}_{10}(\text{Fe,Zn})_2(\text{Sb,As})_4\text{S}_{13}$ fahlores. It is inferred that miscibility gaps in $(\text{Cu,Ag})_{10}(\text{Fe,Zn})_2\text{As}_4\text{S}_{13}$ fahlores have critical temperatures several °C below those established for their Sb counterparts (170 to 185°C). Depending on the structural role of Ag in arsenian fahlores, critical temperatures for $(\text{Cu,Ag})_{10}(\text{Fe,Zn})_2(\text{Sb,As})_4\text{S}_{13}$ fahlores may vary from comparable to those inferred for $(\text{Cu,Ag})_{10}(\text{Fe,Zn})_2\text{As}_4\text{S}_{13}$ fahlores, if the As for Sb substitution stabilizes Ag in tetrahedral metal sites, to temperatures approaching 370°C, if the As for Sb substitution results in an increase in the site preference of Ag for trigonal-planar metal sites. The latter topology is more likely based on comparison of calculated miscibility gaps with compositions of fahlores from nature exhibiting the greatest departure from the $\text{Cu}_{10}(\text{Fe,Zn})_2(\text{Sb,As})_4\text{S}_{13}$ and $(\text{Cu,Ag})_{10}(\text{Fe,Zn})_2\text{Sb}_4\text{S}_{13}$ planes of the $(\text{Cu,Ag})_{10}(\text{Fe,Zn})_2(\text{Sb,As})_4\text{S}_{13}$ fahlore cube.

DOI: 10.1134/S0869591117050071

INTRODUCTION

Fahlore² is a common constituent of epithermal and mesothermal, polymetallic sulfide ores, and is the principal source of Ag to the mining industry from Ag-Pb-Zn sulfide ore deposits. Fahlore typically approximates the simple formula $(\text{Cu,Ag})_{10}(\text{Fe,Zn})_2(\text{Sb,As})_4\text{S}_{13}$ (for example, Johnson and Jeanloz, 1983) with the vast preponderance of its compositions lying close to the $\text{Cu}_{10}(\text{Fe,Zn})_2(\text{Sb,As})_4\text{S}_{13}$ and $(\text{Cu,Ag})_{10}(\text{Fe,Zn})_2\text{Sb}_4\text{S}_{13}$ faces of the $(\text{Cu,Ag})_{10}(\text{Fe,Zn})_2(\text{Sb,As})_4\text{S}_{13}$ fahlore cube (Fig. 1, for example, Sack et al., 1987; Sack,

1992; Sack and Ebel, 1993). Fahlore has $\bar{I}43m$ space group symmetry with two formula units per unit cell, and its structure is a complex derivative of the sphalerite structure of 32 $(\text{Zn,Fe})\text{S}$ formula units in which 8 of the Zn and Fe atoms are replaced by semimetals Sb and As at the midpoints of the half-diagonals (1/4, 1/4, 1/4, etc.), 20 of the 24 remaining Zn and Fe atoms are replaced by Cu and Ag, 8 sulfurs are removed at 1/8, 1/8, 1/8, etc., and 2 sulfurs are added at the corners and center of the unit cell (Pauling and Newmann, 1934). Its structural formula may be written as:



where 6 of the 10 Cu and Ag atoms coordinate the sulfurs added at the corners and center of the unit cell and are in 3-fold coordination by sulfur, the remaining 4 Cu and Ag atoms, along with 2 Fe and Zn atoms, occupy the tetrahedral metal sites left over from the sphalerite structure, and the semimetals Sb and As are bound to three basal S in a pyramidal arrangement which is characteristic of the sulfosalt mineral group (for example, Pauling and Newmann, 1934; Wuensch, 1964; Wuensch et al., 1966).

Our interest in fahlores derives from its extensive capacity for solid solution, a capacity which extends considerably beyond the $\text{Fe} \leftrightarrow \text{Zn}$, $\text{Sb} \leftrightarrow \text{As}$, and $\text{Cu} \leftrightarrow \text{Ag}$ substitutions, and includes, most common-

¹ The article is published in the original.

² Fahlore is the group name for a $\text{M}_{12}\text{X}_4\text{Y}_{13}$ (where M = Cu, Ag, Fe, Zn, Cd, Mn, Hg; X = As, Sb, Bi, Te; Y = S, Se) family of sulfosalts (for example, Cronstedt, 1758; Ramdohr, 1969; Gaines et al., 1977; Mosgova and Tsepin, 1983; Spiridonov, 1984; Spiridonov and Okrugin, 1985; Ebel and Sack, 1989; Sack et al., 2005) whose limiting compositions, endmembers, varieties, and compositional species have been designated by a plethora of officially, and sometimes commonly, recognized terms including binnite or tennantite (Cu-, Fe-, and As-rich fahlore), giraudite (Cu-, Zn-, and As-rich fahlore), freibergite (Ag-, Fe-, and Sb-rich fahlore), hakite (Cu-, Hg-, and Sb-rich fahlore), tetrahedrite (Cu-, Fe-, and Sb-rich fahlore), goldfieldite (Cu- and Te-rich fahlore), and many others (compare, Gaines et al., 1977; Spiridonov, 1984). For obvious reasons we prefer to use the group name fahlore with appropriate chemical descriptors when discussing the thermochemistry of this solid solution.

ly, the $\text{Fe} \Leftrightarrow \text{Mn}$, $\text{Fe} \Leftrightarrow \text{Cd}$, $\text{Fe} \Leftrightarrow \text{Hg}$, $\text{S} \Leftrightarrow \text{Se}$, $2\text{Fe} \Leftrightarrow \text{CuFe}^{3+}$, $\text{FeSb} \Leftrightarrow \text{CuTe}$, and $\text{CuSb} \Leftrightarrow \text{Te}$ substitutions, as well as substitutions that incorporate Bi, Co, Sn, Ge, Ga, and In into the fahlore structure (for example, Hall, 1972; Charlat and Levy, 1974, 1975; Spiridonov and Okrugin, 1985; Makovicky and Karop-Møller, 1994; Breskovska and Tartan, 1994; Klünder-Hansen et al., 2003a, 2003b; Karop-Møller and Makovicky, 2003; Makovicky, 2006). This capacity for solid solution makes fahlore a potentially ideal petrogenetic indicator of ore-forming processes, events and parameters, particularly if original fahlore (and associated sulfide solutions) compositions are preserved or may be reconstructed (for example, Sack et al. 2002, 2005). And this extensive capacity for solid solution is often expressed in zoning in fahlore compositions on district scales in both time and space (for example, Goodell, 1970; Wu and Petersen, 1977; Bushnell, 1983; Lynch, 1989, Sack and Goodell, 2002; Sack et al., 2003; Sack and Lichtner, 2009, 2010), zoning that may be rationalized given comprehensive thermodynamic, kinetic, and reactive transport models for hydrothermal fluids, fahlore and coexisting sulfides, oxides and silicates. Indeed, it is anticipated that such models would lead to the development of new methods of mineral exploration and resource evaluation that would complement, if not replace, the primitive statistical constructs currently employed. It is towards this objective that we review and refine a thermodynamic model for fahlores.

The thermodynamics of $(\text{Cu,Ag})_{10}(\text{Fe,Zn})_2(\text{Sb,As})_4\text{S}_{13}$ fahlores have been formulated and calibrated based on experimental and petrological findings (for example, O'Leary and Sack, 1987; Sack et al., 1987; Sack, 1992, 2000, 2005; Sack et al., 2003; Sack and Lichtner, 2009, 2010). Calibrations for its thermodynamic properties have gone through several cycles of database development, both for it, and for coexisting sulfides and sulfosalts. This thermochemical database development has resulted in models for the thermodynamic properties of $(\text{Cu,Ag})_{10}(\text{Fe,Zn})_2\text{Sb}_4\text{S}_{13}$ fahlores that are demonstrably consistent with observed phenomena (for example, Hernández and Akasaka, 2007, 2010), as exemplified by the recent confirmations of miscibility gaps in fahlores from Ag–Pb–Zn deposits (Sack et al., 2003; Chinchilla et al., 2016) first predicted by O'Leary and Sack (1987), and correct predictions of sulfide ore-forming assemblages and primary phase compositions during hydrothermal ore deposition in the Coeur d'Alene mining district of northern Idaho, USA and the Keno Hill mining district in the Yukon territory, Canada (Sack and Lichtner, 2009, 2010).

In contrast, the thermodynamic properties of fahlores on the $(\text{Cu,Ag})_{10}(\text{Fe,Zn})_2\text{As}_4\text{S}_{13}$ face and in the interior of the fahlore cube are less well known. In particular, the Gibbs energies of the As-bearing vertices are unknown and the nonideality associated with the As for Sb substitution is only loosely constrained (Sack and Ebel, 1993). In addition, although the

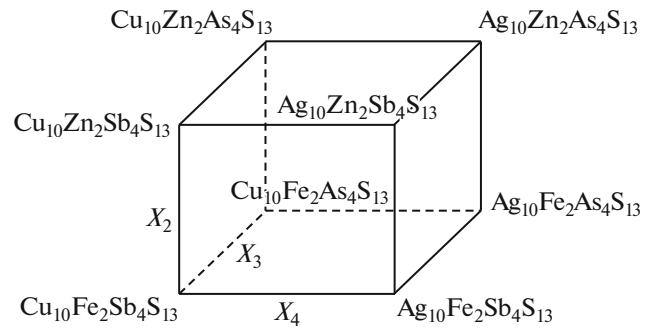


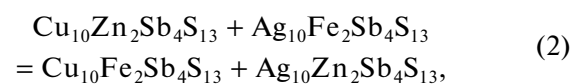
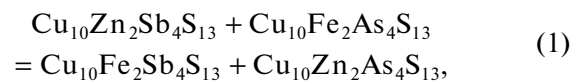
Fig. 1. The $(\text{Cu,Ag})_{10}(\text{Fe,Zn})_2(\text{Sb,As})_4\text{S}_{13}$ fahlore cube with $X_2 = \text{Zn}/(\text{Zn}+\text{Fe})$, $X_3 = \text{As}/(\text{As}+\text{Sb})$, and $X_4 = \text{Ag}/(\text{Ag}+\text{Cu})$.

structural role of Ag has now been established for Sb fahlores (that is, the front face of the fahlore cube; for example, Kalbskopf, 1972; Peterson and Miller, 1986; O'Leary and Sack, 1987; Charnock et al., 1988, 1989; Sack et al., 2003; Sack 2005), it has not been similarly constrained for arsenian fahlores (for example, Johnson and Burnham, 1985).

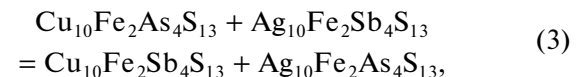
In this paper we outline the predictions of the most recent calibration of fahlore thermodynamic mixing parameters (Sack, 2005) regarding miscibility gaps in the $(\text{Cu,Ag})_{10}(\text{Fe,Zn})_2(\text{Sb,As})_4\text{S}_{13}$ fahlore cube. We demonstrate that these predicted miscibility gaps are consistent with the compositions of fahlores found in polymetallic sulfide ore deposits. We then examine how these gaps would be modified by adjustments in the two thermodynamic mixing parameters that are presently either loosely constrained or unconstrained. It is hoped that these efforts will help encourage and guide petrological studies to find evidence for miscibility gaps in arsenian fahlores, with the aim of further refining the Gibbs energy surface of this remarkable petrogenetic indicator.

THERMODYNAMIC FORMULATION

Experimental and petrological studies have documented that Zn and As, Zn and Ag, and As and Ag are incompatible in the fahlore structure (for example, Raabe and Sack, 1984; Sack and Loucks, 1985; O'Leary and Sack, 1987; Ebel and Sack, 1989, 1991; Sack, 2002; Sack et al., 2003; Sack and Brackebusch, 2004). These incompatibilities are expressed in positive Gibbs energies of the reciprocal reactions



and



reactions relating the vertices on the left-hand side, front and bottom faces of the fahlore cube of Fig. 1. In a thermodynamic formulation that makes explicit provision for the energies of the reciprocal reactions responsible for these incompatibilities (for example, Sack, 1992, 2005), the thermodynamic state of fahlores in the $(\text{Cu,Ag})_{10}(\text{Fe,Zn})_2(\text{Sb,As})_4\text{S}_{13}$ cube is specified with composition variables:

$$X_2 \equiv \text{Zn}/(\text{Zn} + \text{Fe}), \quad (4)$$

$$X_3 \equiv \text{As}/(\text{As} + \text{Sb}), \quad (5)$$

and

$$X_4 \equiv \text{Ag}/(\text{Ag} + \text{Cu}), \quad (6)$$

and a long-range-ordering variable, s , is used to account for ordering of Ag and Cu between trigonal-planar and tetrahedral metal sites:

$$s \equiv X_{\text{Ag}}^{\text{TRG}} - \frac{3}{2} X_{\text{Ag}}^{\text{TET}}. \quad (7)$$

This choice of composition and ordering variables leads to the following set of equations relating compo-

sition and ordering variables to mole fractions of cations on crystallographically distinct sites (that is, site population equations):

$$X_{\text{Ag}}^{\text{TRG}} = X_4 + \frac{2}{5}s, \quad X_{\text{Cu}}^{\text{TRG}} = (1 - X_4) - \frac{2}{5}s, \quad (8a)$$

$$X_{\text{Ag}}^{\text{TET}} = \frac{2}{3}X_4 - \frac{2}{5}s, \quad X_{\text{Cu}}^{\text{TET}} = \frac{2}{3}(1 - X_4) + \frac{2}{5}s, \quad (8b)$$

$$X_{\text{Zn}}^{\text{TET}} = \frac{1}{3}X_2, \quad X_{\text{Fe}}^{\text{TET}} = \frac{1}{3}(1 - X_2), \quad (8c)$$

$$X_{\text{As}}^{\text{SM}} = X_3, \quad X_{\text{Sb}}^{\text{SM}} = 1 - X_3. \quad (8d)$$

In this formulation a Taylor's expansion of second-degree in the X_2, X_3, X_4 and s variables is used to describe the molar vibrational Gibbs energy, \bar{G}^* . And this expansion produces the following expression for the molar Gibbs energy of $(\text{Cu,Ag})_{10}(\text{Fe,Zn})_2(\text{Sb,As})_4\text{S}_{13}$ fahlores, when Taylor coefficients are identified with thermodynamic parameters (for example, Thompson, 1969, 1970; Sack, 1982, 2014; Sack and Ghiorso, 1991a, 1991b):

$$\begin{aligned} \bar{G} = & \bar{G}_1^\circ(X_1) + \bar{G}_2^\circ(X_2) + \bar{G}_3^\circ(X_3) + \bar{G}_4^\circ(X_4) + \bar{G}_1^*(s) + \Delta\bar{G}_{23}^\circ(X_2)(X_3) \\ & + \Delta\bar{G}_{24}^\circ(X_2)(X_4) + \Delta\bar{G}_{34}^\circ(X_3)(X_4) + W_{\text{FeZn}}^{\text{TET}}(X_2)(1 - X_2) + W_{\text{AsSb}}^{\text{SM}}(X_3)(1 - X_3) \\ & + \Delta\bar{G}_{2s}^*(X_2)(s) + \Delta\bar{G}_{3s}^*(X_3)(s) + \frac{1}{10}(\Delta\bar{G}_{4s}^* - 4W_{\text{AgCu}}^{\text{TRG}} + 6W_{\text{AgCu}}^{\text{TET}})(2X_4 - 1)(s) \\ & + (\Delta\bar{G}_{4s}^* + W_{\text{AgCu}}^{\text{TRG}} + W_{\text{AgCu}}^{\text{TET}})(X_4)(1 - X_4) + \frac{1}{25}(6\Delta\bar{G}_{4s}^* - 4W_{\text{AgCu}}^{\text{TRG}} - 9W_{\text{AgCu}}^{\text{TET}})(s)^2 \\ & + RT \left[\ln \left[\left(\frac{3}{2} \right)^4 (3)^2 \right] + 2X_2 \ln(X_2/3) + 2(1 - X_2) \ln((1 - X_2)/3) + 4X_3 \ln(X_3) \right. \\ & + 4(1 - X_3) \ln(1 - X_3) + 6 \left(X_4 + \frac{2}{5}s \right) \ln \left(X_4 + \frac{2}{5}s \right) + 6 \left(1 - X_4 - \frac{2}{5}s \right) \ln \left(1 - X_4 - \frac{2}{5}s \right) \\ & \left. + 6 \left(\frac{2}{3}X_4 - \frac{2}{5}s \right) \ln \left(\frac{2}{3}X_4 - \frac{2}{5}s \right) + 6 \left(\frac{2}{3}(1 - X_4) + \frac{2}{5}s \right) \ln \left(\frac{2}{3}(1 - X_4) + \frac{2}{5}s \right) \right], \end{aligned} \quad (9)$$

when we utilize the relationship between molar Gibbs energy, vibrational Gibbs energy, and configurational entropy (\bar{S}^{IC}):

$$\bar{G} = \bar{G}^* - T\bar{S}^{\text{IC}}, \quad (10)$$

utilize the site population equations in the expression for \bar{S}^{IC} :

$$\begin{aligned} \bar{S}^{\text{IC}} = & -R \left[6(X_{\text{Zn}}^{\text{TET}}) \ln(X_{\text{Zn}}^{\text{TET}}) + 6(X_{\text{Fe}}^{\text{TET}}) \ln(X_{\text{Fe}}^{\text{TET}}) \right. \\ & + 4(X_{\text{As}}^{\text{SM}}) \ln(X_{\text{As}}^{\text{SM}}) + 4(X_{\text{Sb}}^{\text{SM}}) \ln(X_{\text{Sb}}^{\text{SM}}) + 6(X_{\text{Ag}}^{\text{TRG}}) \ln(X_{\text{Ag}}^{\text{TRG}}) \\ & \left. + 6(X_{\text{Cu}}^{\text{TRG}}) \ln(X_{\text{Cu}}^{\text{TRG}}) + 6(X_{\text{Ag}}^{\text{TET}}) \ln(X_{\text{Ag}}^{\text{TET}}) + 6(X_{\text{Cu}}^{\text{TET}}) \ln(X_{\text{Cu}}^{\text{TET}}) \right], \end{aligned} \quad (11)$$

and recognize that

$$X_1 = 1 - X_2 - X_3 - X_4, \quad (12)$$

where X_1 is the mole fraction of the basis component $\text{Cu}_{10}\text{Fe}_2\text{Sb}_4\text{S}_{13}^3$. The thermodynamic param-

eters in Eq. (9) are (1) the molar Gibbs energies of the endmember components ($\bar{G}_1^\circ, \bar{G}_2^\circ, \bar{G}_3^\circ$, and \bar{G}_4°), (2) the Gibbs energies of reciprocal reactions (1), (2), and (3) ($\Delta\bar{G}_{23}^\circ, \Delta\bar{G}_{24}^\circ$, and $\Delta\bar{G}_{34}^\circ$), (3) symmetric regular solution parameters describing the nonideality of mixing of Ag and Cu on trigonal-planar metal sites ($W_{\text{AgCu}}^{\text{TRG}}$), of Ag and Cu, and of Fe and

³ It is important to note that X_1 may have negative values, having the value of -1 in the vertices $\text{Cu}_{10}\text{Zn}_2\text{As}_4\text{S}_{13}$, $\text{Ag}_{10}\text{Zn}_2\text{Sb}_4\text{S}_{13}$ and $\text{Ag}_{10}\text{Fe}_2\text{As}_4\text{S}_{13}$, and, -2 in the vertex $\text{Ag}_{10}\text{Zn}_2\text{As}_4\text{S}_{13}$.

Zn, on tetrahedral metal sites ($W_{\text{AgCu}}^{\text{TET}}$ and $W_{\text{FeZn}}^{\text{TET}}$), vibrational Gibbs energy of the Ag-Cu ordering reaction and of As and Sb on semimetal sites ($W_{\text{AsSb}}^{\text{SM}}$), (4) the action ($\Delta\bar{G}_s^*$):

$$\begin{aligned} & \frac{1}{2}\text{Cu}_6^{\text{TRG}}(\text{Ag}_{2/3}, \text{Fe}_{1/3})_6^{\text{TET}}\text{Sb}_4\text{S}_{13} + \frac{1}{10}\text{Ag}_{10}\text{Fe}_2\text{Sb}_4\text{S}_{13} \\ & = \frac{1}{2}\text{Ag}_6^{\text{TRG}}(\text{Cu}_{2/3}, \text{Fe}_{1/3})_6^{\text{TET}}\text{Sb}_4\text{S}_{13} + \frac{1}{10}\text{Cu}_{10}\text{Fe}_2\text{Sb}_4\text{S}_{13}, \end{aligned} \quad (13)$$

and (5) the vibrational Gibbs energies of reciprocal ordering reactions $\Delta\bar{G}_{2s}^*$, $\Delta\bar{G}_{3s}^*$, and $\Delta\bar{G}_{4s}^*$:

$$\begin{aligned} & \frac{1}{2}\text{Cu}_6^{\text{TRG}}(\text{Ag}_{2/3}, \text{Zn}_{1/3})_6^{\text{TET}}\text{Sb}_4\text{S}_{13} + \frac{1}{10}\text{Cu}_{10}\text{Fe}_2\text{Sb}_4\text{S}_{13} \\ & + \frac{1}{2}\text{Ag}_6^{\text{TRG}}(\text{Cu}_{2/3}, \text{Fe}_{1/3})_6^{\text{TET}}\text{Sb}_4\text{S}_{13} + \frac{1}{10}\text{Ag}_{10}\text{Zn}_2\text{Sb}_4\text{S}_{13} \\ & = \frac{1}{2}\text{Ag}_6^{\text{TRG}}(\text{Cu}_{2/3}, \text{Zn}_{1/3})_6^{\text{TET}}\text{Sb}_4\text{S}_{13} + \frac{1}{10}\text{Ag}_{10}\text{Fe}_2\text{Sb}_4\text{S}_{13} \\ & + \frac{1}{2}\text{Cu}_6^{\text{TRG}}(\text{Ag}_{2/3}, \text{Fe}_{1/3})_6^{\text{TET}}\text{Sb}_4\text{S}_{13} + \frac{1}{10}\text{Cu}_{10}\text{Zn}_2\text{Sb}_4\text{S}_{13}, \end{aligned} \quad (14)$$

$$\begin{aligned} & \frac{1}{2}\text{Cu}_6^{\text{TRG}}(\text{Ag}_{2/3}, \text{Fe}_{1/3})_6^{\text{TET}}\text{As}_4\text{S}_{13} + \frac{1}{10}\text{Cu}_{10}\text{Fe}_2\text{Sb}_4\text{S}_{13} \\ & + \frac{1}{2}\text{Ag}_6^{\text{TRG}}(\text{Cu}_{2/3}, \text{Fe}_{1/3})_6^{\text{TET}}\text{Sb}_4\text{S}_{13} + \frac{1}{10}\text{Ag}_{10}\text{Fe}_2\text{As}_4\text{S}_{13} \\ & = \frac{1}{2}\text{Ag}_6^{\text{TRG}}(\text{Cu}_{2/3}, \text{Fe}_{1/3})_6^{\text{TET}}\text{As}_4\text{S}_{13} + \frac{1}{10}\text{Ag}_{10}\text{Fe}_2\text{Sb}_4\text{S}_{13} \\ & + \frac{1}{2}\text{Cu}_6^{\text{TRG}}(\text{Ag}_{2/3}, \text{Fe}_{1/3})_6^{\text{TET}}\text{Sb}_4\text{S}_{13} + \frac{1}{10}\text{Cu}_{10}\text{Fe}_2\text{As}_4\text{S}_{13}, \end{aligned} \quad (15)$$

and

$$\begin{aligned} & \text{Cu}_{10}\text{Fe}_2\text{Sb}_4\text{S}_{13} + \text{Ag}_{10}\text{Fe}_2\text{Sb}_4\text{S}_{13} \\ & = \text{Ag}_6^{\text{TRG}}(\text{Cu}_{2/3}, \text{Fe}_{1/3})_6^{\text{TET}}\text{Sb}_4\text{S}_{13} + \text{Cu}_6^{\text{TRG}}(\text{Ag}_{2/3}, \text{Fe}_{1/3})_6^{\text{TET}}\text{Sb}_4\text{S}_{13}. \end{aligned} \quad (16)$$

The values of these parameters are given in Table 1. The ordering variable is evaluated by setting

$$\left(\frac{\partial\bar{G}}{\partial s}\right)_{T, X_2, X_3, X_4} = 0, \quad (17)$$

which results in the following condition of homogeneous equilibrium:

$$\begin{aligned} 0 = & RT \ln \frac{\left(X_4 + \frac{2}{5}s\right)\left(\frac{2}{3}[1 - X_4] + \frac{2}{5}s\right)}{\left(1 - X_4 - \frac{2}{5}s\right)\left(\frac{2}{3}X_4 - \frac{2}{5}s\right)} + \frac{5}{12}(\Delta\bar{G}_s^* + \Delta\bar{G}_{2s}^*(X_2) + \Delta\bar{G}_{3s}^*(X_3)) \\ & + \frac{1}{24}(\Delta\bar{G}_{4s}^* + 6W_{\text{AgCu}}^{\text{TET}} - 4W_{\text{AgCu}}^{\text{TRG}})(2X_4 - 1) + \frac{1}{30}(6\Delta\bar{G}_{4s}^* - 9W_{\text{AgCu}}^{\text{TET}} - 4W_{\text{AgCu}}^{\text{TRG}})(s). \end{aligned} \quad (18)$$

Finally, chemical potentials of the vertices of the fahlore composition-ordering space may be evaluated from the equation:

$$\mu_j = \bar{G} + \sum_{i=1}^4 n_{ij}(1 - X_i) \left(\frac{\partial\bar{G}}{\partial X_i}\right)_{T, X_k/X_l} + (s_j - s) \left(\frac{\partial\bar{G}}{\partial s}\right)_{T, X_2, X_3, X_4}, \quad (19)$$

n_{ij}

where the n_i coefficients are the mole fractions of the i components ($\text{Cu}_{10}\text{Fe}_2\text{Sb}_4\text{S}_{13}$, $\text{Cu}_{10}\text{Zn}_2\text{Sb}_4\text{S}_{13}$, $\text{Cu}_{10}\text{Fe}_2\text{Sb}_4\text{S}_{13}$, and $\text{Ag}_{10}\text{Fe}_2\text{As}_4\text{S}_{13}$), and s_j is the value

of s (-1 , 0 or $+1$), in the j vertex of composition-ordering space of interest (compare Sack, 1982; Ghiorsso, 1990). Explicit expressions for the j components

with $s_j = 0$ are given in Sack et al. (1987; Table 1). Corresponding expressions for j components with $s = -1$ and $+1$ are left to be derived by the interested reader⁴

Limiting the Taylor's expansion to second-degree implies some relationships between possible thermodynamic parameters that are related through various symmetry operations. One such relationship is between the molar Gibbs energies of the vertices of the fahlore cube. Only seven of these are independent,

$$\bar{G}_{\text{Ag}_{10}\text{Zn}_2\text{As}_4\text{S}_{13}}^{\circ} = \bar{G}_1^{\circ} + (\bar{G}_{\text{Ag}_{10}\text{Fe}_2\text{As}_4\text{S}_{13}}^{\circ} - \bar{G}_2^{\circ}) + (\bar{G}_{\text{Ag}_{10}\text{Zn}_2\text{Sb}_4\text{S}_{13}}^{\circ} - \bar{G}_3^{\circ}) + (\bar{G}_{\text{Cu}_{10}\text{Zn}_2\text{As}_4\text{S}_{13}}^{\circ} - \bar{G}_4^{\circ}). \quad (24)$$

Three additional requirements are that the nonideality associated with the Zn for Fe, As for Sb, and Ag for Cu substitutions is invariant with respect to the extent of operation of the other substitutions. These simplifications were deemed necessary given the constraints currently available, but they could be readily relaxed should a more comprehensive dataset require so in the future.

Thermodynamic Model

The present thermodynamic model for $(\text{Cu,Ag})_{10}(\text{Fe,Zn})_2(\text{Sb,As})_4\text{S}_{13}$ fahlores is most rigorously constrained near the $(\text{Cu,Ag})_{10}(\text{Fe,Zn})_2\text{Sb}_4\text{S}_{13}$ front, $\text{Cu}_{10}(\text{Fe,Zn})_2(\text{Sb,As})_4\text{S}_{13}$ side and $(\text{Cu,Ag})_{10}\text{Fe}_2(\text{Sb,As})_4\text{S}_{13}$ bottom faces of the fahlore cube by results of experimental and petrological studies of the Fe-Zn exchange reaction between

⁴ The need for negative mole fractions in the description of reciprocal solutions is obvious. If, for example, we were to limit ourselves to only positive mole fractions of the basis component $\text{Cu}_{10}\text{Fe}_2\text{Sb}_4\text{S}_{13}$ in our formulation, then we could only treat one quarter of the composition space of the fahlore cube with such a formulation (that is, the volume between the $\text{Cu}_{10}\text{Fe}_2\text{Sb}_4\text{S}_{13}$ vertex and the diagonal plane passing through the $\text{Cu}_{10}\text{Zn}_2\text{Sb}_4\text{S}_{13}$, $\text{Cu}_{10}\text{Fe}_2\text{As}_4\text{S}_{13}$, and $\text{Ag}_{10}\text{Fe}_2\text{Sb}_4\text{S}_{13}$ vertices), and would need to formulate three more models with different definitions of mole fractions to treat the full volume of the cube. And, of course we would have to make sure that the parameters governing nonideal interactions along the lines and within the planes that these four geometric volumes would share were "internally consistent" with each other. Some of the difficulties with such formulations may be illustrated for a simpler reciprocal solution, $(\text{Mg,Fe})[\text{Al,Cr}]_2\text{O}_4$ spinels, an illustration further simplified assuming complete ordering of Mg and Fe into tetrahedral sites, (), and Al and Cr into octahedral sites, [], (a reasonable first approximation; for example, Sack, 1982, 2014), and that Mg and Fe, and Al and Cr, mix ideally (poor approximations; for example, Sack and Ghiorso, 1991a, 1991b).

If we define $X_2 = \text{Mg}/(\text{Mg}+\text{Fe})$ and $X_3 = \text{Cr}/(\text{Cr}+\text{Al})$, and only consider positive mole fractions of the endmember components (that is, treat $\text{FeAl}_2\text{O}_4(1)$ – $\text{MgAl}_2\text{O}_4(2)$ – $\text{FeCr}_2\text{O}_4(3)$ spinels as a ternary solution) we would write the following expression for G :

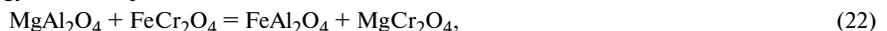
$$\bar{G} = \bar{G}_1^{\circ}(X_1) + \bar{G}_2^{\circ}(X_2) + \bar{G}_3^{\circ}(X_3) + W_{23}(X_2)(X_3) + RT [X_2 \ln(X_2) + (1 - X_2) \ln(1 - X_2) + 2X_3 \ln(X_3) + 2(1 - X_3) \ln(1 - X_3)], \quad (20)$$

if we account for the fact that the $\text{Mg}(\text{Fe})_{-1}$ exchange potential, $\mu_{\text{Mg}(\text{Fe})_{-1}}^{\text{SP}}$, is roughly linearly dependent on X_3 at a given temperature and pressure (for example, Evans and Frost, 1975; Sack, 1982; Engi, 1983; Sack and Ghiorso, 1991b) with a symmetric regular solution parameter W_{23} . To treat the other half of the composition plane defined by the $\text{MgCr}_2\text{O}_4(4)$ – $\text{FeCr}_2\text{O}_4(3)$ – $\text{MgAl}_2\text{O}_4(2)$ components with positive mole fractions in a similar fashion, we would then write:

$$\begin{aligned} \bar{G} = & \bar{G}_4^{\circ}(X_1') + \bar{G}_3^{\circ}(X_2') + \bar{G}_2^{\circ}(X_3') + W_{23}'(X_2')(X_3') + RT \left[X_2' \ln(X_2') \right. \\ & \left. + (1 - X_2') \ln(1 - X_2') + 2X_3' \ln(X_3') + 2(1 - X_3') \ln(1 - X_3') \right], \end{aligned} \quad (21)$$

where, to render these two separate treatments consistent, it would be necessary to recognize that $X_1' = -X_1$, $X_2' = (1 - X_2)$, $X_3' = (1 - X_3)$,

$W_{23}' = -W_{23}$ and that W_{23} is the Gibbs energy of the reciprocal reaction



$\Delta\bar{G}_{23}^{\circ}$, facts that may be readily established by recognizing that

$$\mu_{\text{Mg}(\text{Fe})_{-1}}^{\text{SP}} = \left(\frac{\partial \bar{G}}{\partial X_2} \right)_{T,P,X_3} = - \left(\frac{\partial \bar{G}}{\partial X_2'} \right)_{T,P,X_3'}. \quad (23)$$

Of course, relaxing the assumptions that Mg and Fe and Al and Cr mix ideally and making explicit provision for the ordering of Mg^{2+} , Fe^{2+} , and Al^{3+} between tetrahedral and octahedral sites through two conditions of homogeneous equilibrium, would make the process of discovery of the relationships between parameters for the two ternary subsystems (with positive mole fractions of their endmember components) required to make these formulations "internally consistent", at best, a significantly more daunting task, if achievable at all. And then to consider expanding this type of approach to the case of fahlores or even more complex reciprocal solutions such as biotite and hornblende would be unworkable, as it would mean progressively smaller percentages of the composition-ordering spaces would be treated with each constituent subspace with positive mole fractions and progressively more relationships between parameters of these constituent subspaces would have to be discovered to render them "internally consistent" with each other.

fahlore and (Zn,Fe) sphalerite (for example, Raabe and Sack, 1984; Sack and Loucks, 1985; O'Leary and Sack, 1987) and the Ag-Cu exchange reaction between fahlore and an assemblage fixing the $\text{Ag}(\text{Cu})_{-1}$ exchange potential, pyrite, chalcopyrite, and electrum of fixed Ag/Au ratios (for example, Ebel and Sack, 1989, 1991). Calibrations of the parameters of this thermodynamic model were subsequently improved based on experimental, theoretical and field studies **studies** of fahlore and associated sulfides (for example, Harlov and Sack, 1994; Ghosal and Sack, 1995, 1999; Balabin and Sack, 2000; Sack, 2000, 2002, 2005; Sack et al., 2002, 2003, 2005; Sack and Brackebusch, 2004; Chutas and Sack, 2004; Chutas et al., 2008). Estimates for the Gibbs energy of formation of the endmember vertices of the $(\text{Cu,Ag})_{10}(\text{Fe,Zn})_2\text{Sb}_4\text{S}_{13}$ face were subsequently obtained which satisfy the rigorous field tests posed by sulfide ores from Ag–Pb–Zn mining districts in Coeur d'Alene, ID, USA and Keno Hill, Yukon, Canada (Sack and Lichtner, 2009, 2010).

The resulting model is very similar to that produced by O'Leary and Sack (1987) with regard to its predictions of miscibility gaps on the front face of the fahlore cube (Figs. 2, 3). The critical curves for $(\text{Cu,Ag})_{10}(\text{Fe,Zn})_2\text{Sb}_4\text{S}_{13}$ fahlores are only marginally lowered in temperature (by less than 5°C), and the spacing between $(\text{Cu,Ag})_{10}\text{Zn}_2\text{Sb}_4\text{S}_{13}$ and $(\text{Cu,Ag})_{10}\text{Fe}_2\text{Sb}_4\text{S}_{13}$ miscibility gaps is slightly compressed in Ag/(Ag + Cu). These modifications are a result of implementing the CVM model of (Zn,Fe)S sphalerite thermodynamics of Balabin and Sack (2000) into the analysis of sphalerite-fahlore Fe-Zn exchange equilibria, and, of other adjustments made to accommodate subsequent field studies and database development. And, as previously noted, both these, and the previously predicted, miscibility gaps are within analytical uncertainty of miscibility gaps observed in natural fahlores for temperatures corroborated by mineral assemblages and fluid inclusions (for example, Sack et al., 2003, Fig. 6; Chinchilla et al., 2016, Fig. 16). A modest downward adjustment to the estimate for the Gibbs energy of the reciprocal reaction expressing the incompatibility between As and Ag, $\Delta\bar{G}_{34}^{\circ}$, was also motivated by these studies. Finally, the model predicts miscibility gaps for fahlores inside the cube that are in better agreement with the distribution of natural fahlores furthest from the $\text{Cu}_{10}(\text{Fe,Zn})_2(\text{Sb,As})_4\text{S}_{13}$ and $(\text{Cu,Ag})_{10}(\text{Fe,Zn})_2\text{Sb}_4\text{S}_{13}$ faces of the fahlore cube (compare Fig. 4).

ADJUSTMENTS TO THERMODYNAMIC PARAMETERS

The parameters $W_{\text{AsSb}}^{\text{SM}}$ and $\Delta\bar{G}_{3s}^*$ may be adjusted to examine other possible topologies of miscibility gaps within the fahlore cube. Adjustment of $\Delta\bar{G}_{3s}^*$ is more productive, as adjustments in $W_{\text{AsSb}}^{\text{SM}}$ are ineffective

Table 1. Values of thermodynamic mixing parameters

Parameter	Value, kJ/gfw
$\Delta\bar{G}_{23}^{\circ}$	10.84
$\Delta\bar{G}_{24}^{\circ}$	9.00
$\Delta\bar{G}_{34}^{\circ 1}$	50.265
$\Delta\bar{G}_{34}^{\circ 2}$	61.817
$\Delta\bar{G}_s^*$	-1.6736
$\Delta\bar{G}_{2s}^*$	9.00
$\Delta\bar{G}_{3s}^* 1$	0.00
$\Delta\bar{G}_{3s}^* 2$	-10
$\Delta\bar{G}_{4s}^*$	-10.88
$W_{\text{FeZn}}^{\text{TET}}$	0.00
$W_{\text{AsSb}}^{\text{SM}}$	16.74
$W_{\text{AgCu}}^{\text{TET}} \text{TRG}$	0.00
$W_{\text{AgCu}}^{\text{TET}}$	29.01

¹ Initial values for $\Delta\bar{G}_{34}^{\circ}$ and $\Delta\bar{G}_{3s}^*$, with $\Delta\bar{G}_{34}^{\circ}$ ($\Delta\bar{G}_{3s}^*$) given by the relationship illustrated in Fig. 6. ² Tentative final values.

and problematic. Downwards adjustments in $W_{\text{AsSb}}^{\text{SM}}$ might be favored to narrow the gaps in Fig. 4, but such adjustments only marginally narrow the calculated miscibility gaps towards the center of the fahlore cube. The large Gibbs energy of reciprocal reaction (3) is sufficient to insure that these gaps are still more extensive, and extend to higher temperatures than those on the $(\text{Cu,Ag})_{10}(\text{Fe,Zn})_2\text{As}_4\text{S}_{13}$ and $(\text{Cu,Ag})_{10}(\text{Fe,Zn})_2\text{Sb}_4\text{S}_{13}$ faces of the fahlore cube, and the miscibility gaps on these faces are unaltered by adjustments in $W_{\text{AsSb}}^{\text{SM}}$. Such adjustments may also be considered inadvisable.

Although the current estimate of $W_{\text{AsSb}}^{\text{SM}}$ (Table 1) is near the upper bound permitted by experimental constraints on the As–Sb exchange reactions between fahlore and $\text{CuPb}(\text{Sb,As})\text{S}_3$ bournonite-seligmannite solid solutions (Sack and Ebel, 1993), it is below that defined by the correlation of $W_{\text{AsSb}}^{\text{SM}}$ with semimetal/(semimetal + metal) ratios established for coexisting Ag-sulfosalts polybasite-pearceite $[(\text{Ag,Cu})_{16}(\text{Sb,As})_2\text{S}_{11}]$, pyrrargyrite-proustite $[(\text{Ag,Cu})_3(\text{Sb,As})\text{S}_3]$, and miargyrite-

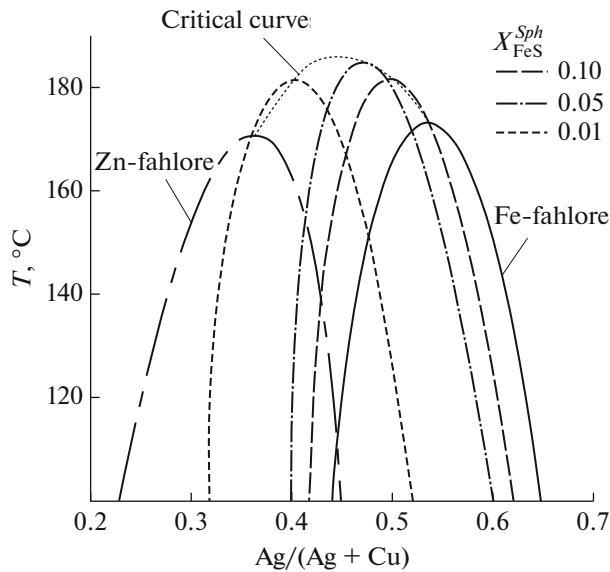


Fig. 2. Calculated temperature—Ag/(Ag+Cu) relations of miscibility gaps in $(\text{Cu},\text{Ag})_{10}\text{Fe}_2\text{Sb}_4\text{S}_{13}$, $(\text{Cu},\text{Ag})_{10}\text{Zn}_2\text{Sb}_4\text{S}_{13}$, and $(\text{Cu},\text{Ag})_{10}(\text{Fe},\text{Zn})_2\text{Sb}_4\text{S}_{13}$ fahlores in Fe—Zn exchange equilibrium with sphalerites with $X_{\text{FeS}}^{\text{Sph}} = 0.01, 0.05,$ and 0.10 . Fe—Zn partitioning between $(\text{Cu},\text{Ag})_{10}(\text{Fe},\text{Zn})_2\text{Sb}_4\text{S}_{13}$ fahlores and $(\text{Zn},\text{Fe})\text{S}$ sphalerites calculated using the parameter values \bar{G} given in Table 1, the expression for \bar{G}^{EX} of $(\text{Zn},\text{Fe})\text{S}$ sphalerite given by Balabin and Sack (2000, p. 937), and the value for the Gibbs energy of the Fe—Zn exchange reaction between $(\text{Zn},\text{Fe})\text{S}$ sphalerites and $\text{Cu}_{10}(\text{Fe},\text{Zn})_2\text{Sb}_4\text{S}$ fahlores given by Sack (2005). Dotted curve is the critical curve for $(\text{Cu},\text{Ag})_{10}(\text{Fe},\text{Zn})_2\text{Sb}_4\text{S}_{13}$ fahlores.

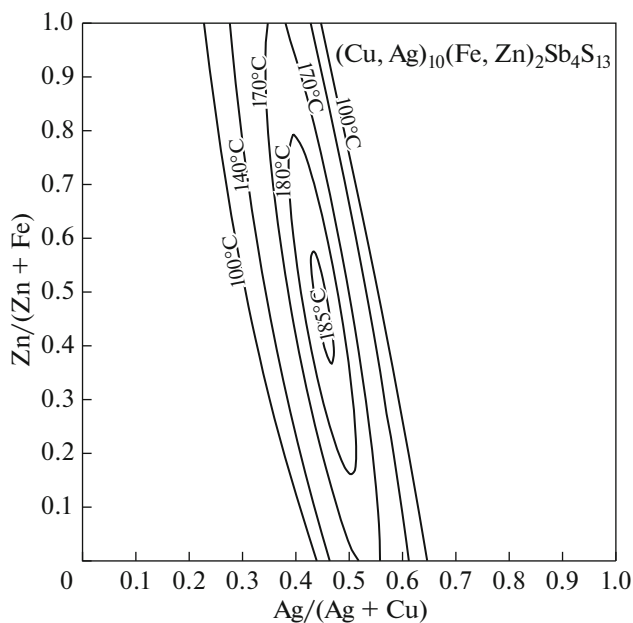
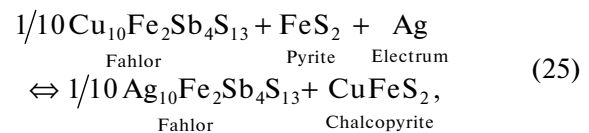


Fig. 3. Calculated 100, 140, 170, 180, and 185°C miscibility gaps for $(\text{Cu},\text{Ag})_{10}(\text{Fe},\text{Zn})_2\text{Sb}_4\text{S}_{13}$ fahlores using parameter values in Table 1.

smithite $[(\text{Ag},\text{Cu})(\text{Sb},\text{As})\text{S}_2]$ (Ghosal and Sack, 1995, Fig. 5).

In contrast, adjustments in $\Delta\bar{G}_{3s}^*$ may significantly alter the configuration of miscibility gaps both on the back $(\text{Cu},\text{Ag})_{10}(\text{Fe},\text{Zn})_2\text{As}_4\text{S}_{13}$ face and within the fahlore cube. In fact, making $\Delta\bar{G}_{3s}$ significantly negative might move the binodes of any miscibility gaps in $(\text{Cu},\text{Ag})_{10}(\text{Fe},\text{Zn})_2\text{As}_4\text{S}_{13}$ fahlores to compositions with X_4 between 0.6 and 1.0, much like where there are gaps in the fahlore compositions reported by Gamyani et al. (2001, Fig. 8). This inference is made evident by examining the condition of homogeneous equilibrium, Eq. (18), from which it is evident that decreasing $\Delta\bar{G}_{3s}^*$ increases $X_{\text{Ag}}^{\text{TRG}}$, strongly increasing the preference of Ag for trigonal-planar sites, if negative enough. In such a case the order variable s might closely approach the perimeters of the s - X_4 diagram (Fig. 5) for positive s , corresponding to mixing of Cu and Ag exclusively on trigonal-planar sites for X_4 between 0 and 0.6, and exclusively on tetrahedral sites for X_4 between 0.6 and 1. And, in such a case, the binodes of any miscibility gap would have to be between X_4 of 0.6 and 1, as we have established that mixing of Cu and Ag is virtually ideal on trigonal planar sites ($W_{\text{AgCu}}^{\text{TRG}} = 0$, Table 1) and is substantially non-ideal on tetrahedral sites (that is, $W_{\text{AgCu}}^{\text{TRG}} \gg 0$). And, of course, adjusting $\Delta\bar{G}_{3s}^*$ in the opposite direction (that is, making it positive) would move the miscibility gaps for $(\text{Cu},\text{Ag})_{10}(\text{Fe},\text{Zn})_2\text{As}_4\text{S}_{13}$ fahlores to lower X_4 than those of $(\text{Cu},\text{Ag})_{10}(\text{Fe},\text{Zn})_2\text{Sb}_4\text{S}_{13}$ fahlores, by lowering the range of X_4 over which Ag changes site preference from trigonal-planar to tetrahedral sites (compare Fig. 5).

For internal consistency any adjustment of $\Delta\bar{G}_{3s}^*$ cannot be performed independently of an adjustment of $\Delta\bar{G}_{34}^{\circ}$, because they are related through the condition of equilibrium for the reaction:



and this linkage is provided by the experimental constraints of Ebel and Sack (1989, 1991) on fahlore compositions in this assemblage for various Au/Ag ratios in electrum at 400 and 300°C. It is convenient to write this condition of equilibrium as:

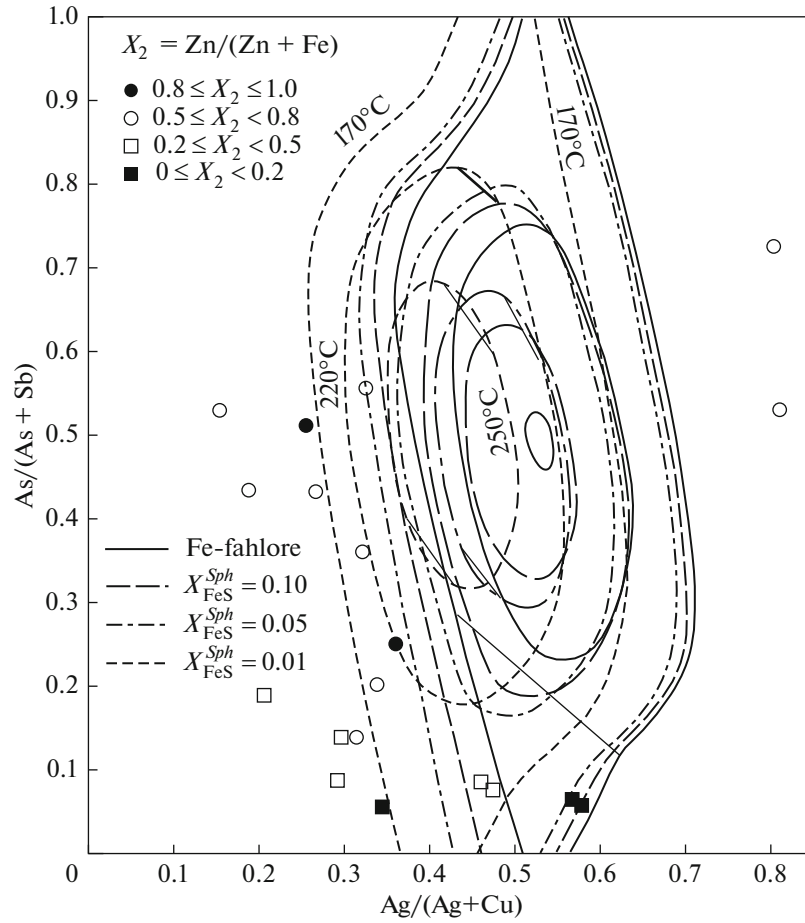


Fig. 4. Calculated miscibility gaps for $(\text{Cu,Ag})_{10}\text{Fe}_2(\text{Sb,As})_4\text{S}_{13}$ fahlores and $(\text{Cu,Ag})_{10}(\text{Fe,Zn})_2(\text{Sb,As})_4\text{S}_{13}$ fahlores in Fe-Zn exchange equilibrium with $(\text{Zn,Fe})\text{S}$ sphalerites with $X_{\text{FeS}}^{\text{Sph}}$ of 0.01, 0.05 and 0.10 for the initial parameter values given in Table 1 (that is, $\Delta\bar{G}_{3s}^* = 0$). Circles and squares are fahlores showing greatest departure from the $\text{Cu}_{10}(\text{Fe,Zn})_2(\text{Sb,As})_4\text{S}_{13}$ and $(\text{Cu,Ag})_{10}(\text{Fe,Zn})_2\text{Sb}_4\text{S}_{13}$ planes of the fahlore cube from the compilations of Sack et al. (1987), Sack (1992), and Sack and Ebel (1993). Thin lines are representative tielines between coexisting fahlores.

$$\begin{aligned}
 \bar{Q}_{X_4}^* &\equiv RT \ln \left[(a_{\text{FeS}_2}^{\text{PYR}}) (a_{\text{Ag}}^{\text{ELEC}}) \right] \\
 &- \frac{1}{10} \left[RT \ln \frac{\left(X_4 + \frac{2}{5}s \right)^6 \left(\frac{2}{3} X_4 - \frac{2}{5}s \right)^4}{\left(1 - X_4 - \frac{2}{5}s \right)^6 \left(\frac{2}{3} [1 - X_4] + \frac{2}{5}s \right)^4} + \Delta\bar{G}_{24}^{\circ}(X_2) \right] \\
 &- \frac{1}{50} \left(\Delta\bar{G}_{4s}^* + 6W_{\text{AgCu}}^{\text{TET}} - 4W_{\text{AgCu}}^{\text{TRG}} \right) (s) - \frac{1}{10} \left(\Delta\bar{G}_{4s}^* + W_{\text{AgCu}}^{\text{TET}} + W_{\text{AgCu}}^{\text{TRG}} \right) (1 - 2X_4) \\
 &= \Delta\bar{G}_{\text{Ag}(\text{Cu})_{-1}}^{\circ} + RT \ln (a_{\text{CuFeS}_2}^{\text{CPY}}) + \frac{1}{10} \Delta\bar{G}_{34}^{\circ}(X_3),
 \end{aligned} \tag{26}$$

where $\Delta\bar{G}_{\text{Ag}(\text{Cu})_{-1}}^{\circ}$ is the standard state Gibbs energy of reaction (25), we may reasonably assume that the activity of FeS_2 in pyrite, $a_{\text{FeS}_2}^{\text{PYR}}$, is unity, we may determine the activity of Ag in electrum, $a_{\text{Ag}}^{\text{ELEC}}$, from the calibration of White et al. (1957), and we may calculate

values of the order parameter s in arsenian fahlores for various assumed values of $\Delta\bar{G}_{3s}^*$ from the condition of homogeneous equilibrium, Eq. (18). We may thus determine $\Delta\bar{G}_{34}^{\circ}$ for a given assumed $\Delta\bar{G}_{3s}^*$ by evaluating the slope of $\bar{Q}_{X_4}^*$ with respect to X_3 at a given $X_{\text{Ag}}^{\text{ELEC}}$.

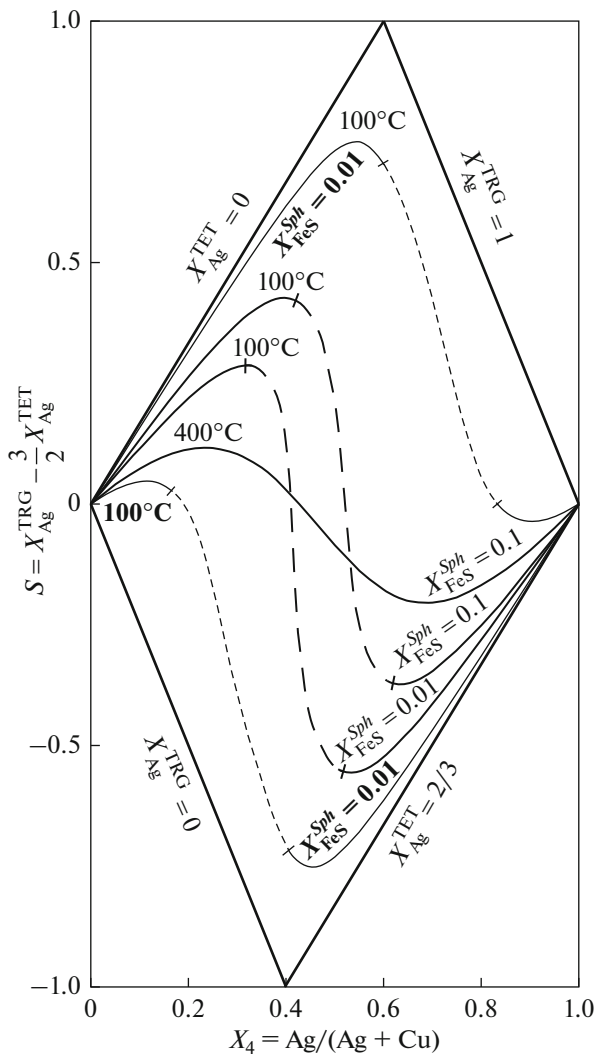


Fig. 5. Ordering variable s – X_4 relations calculated from Eq. (18) for $(\text{Cu,Ag})_{10}(\text{Fe,Zn})_2\text{Sb}_4\text{S}_{13}$ (interior curves) and $(\text{Cu,Ag})_{10}(\text{Fe,Zn})_2\text{As}_4\text{S}_{13}$ (exterior curves) fahlores. $(\text{Cu,Ag})_{10}(\text{Fe,Zn})_2\text{Sb}_4\text{S}_{13}$ fahlores are in Fe–Zn exchange equilibrium with sphalerites with $X_{\text{FeS}}^{\text{Sph}} = 0.1$ (100 and 400°C) and $X_{\text{FeS}}^{\text{Sph}} = 0.01$ (100°C). $(\text{Cu,Ag})_{10}(\text{Fe,Zn})_2\text{As}_4\text{S}_{13}$ fahlores are in Fe–Zn exchange equilibrium with a sphalerite with $X_{\text{FeS}}^{\text{Sph}} = 0.01$ at 100°C for $\Delta\bar{G}_{3s}^* = -10$ (upper curve) and $\Delta\bar{G}_{3s}^* = 10$ kJ/gfw. Dashed portions of curves are for fahlores within calculated miscibility gaps.

However, we cannot determine the value of $\Delta\bar{G}_{\text{Ag}(\text{Cu})-1}^\circ$ from the $X_3 = 0$ intercepts, because the activity of CuFeS_2 in chalcopyrite, $a_{\text{CuFeS}_2}^{\text{CPY}}$, is unknown, as chalcopyrite departs somewhat from stoichiometric CuFeS_2 even in the simple system Cu–Fe–S, where it has a composition of roughly $\text{Cu}_{0.9}\text{Fe}_{1.1}\text{S}_2$, when it is

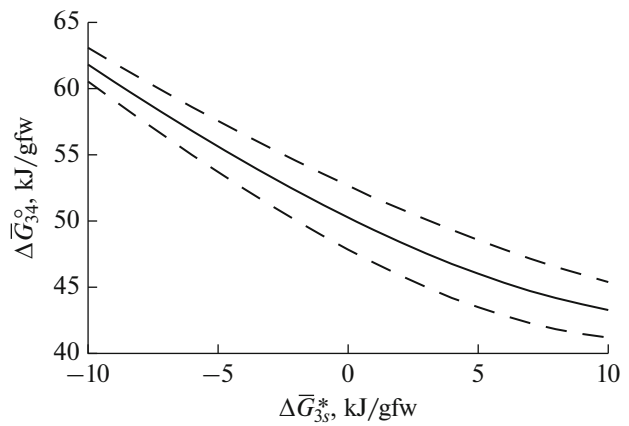
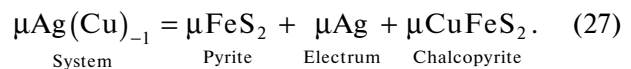


Fig. 6. Values of $\Delta\bar{G}_{34}^\circ$ deduced from the data of Ebel and Sack (1989, 1991) for various assumed values of $\Delta\bar{G}_{3s}^*$. Average values (solid curve) and standard deviations (dashed curves) of $\Delta\bar{G}_{34}^\circ$ are calculated from the mean values of $\Delta\bar{G}_{34}^\circ$ determined from Eq. (26) for the tightest reversal brackets produced from experiments at 300°C and $X_{\text{Ag}}^{\text{ELEC}} = 0.30$, A7-1, C7-1, and S7-1, 300°C and $X_{\text{Ag}}^{\text{ELEC}} = 0.40$, B8-1, D8-2, H8-1, L8-1, M8-1, and S8-1, 400°C and $X_{\text{Ag}}^{\text{ELEC}} = 0.30$, G4-1, I4-1, K4-1, and S4-1, and 400°C and $X_{\text{Ag}}^{\text{ELEC}} = 0.20$, B2-2, D2-3, D2-R1, B2-1, H2-2, J2-2, and S2-1.

saturated with pyrite at 350°C (for example, Cabri, 1973; Sugaki et al., 1975). And its departure from CuFeS_2 stoichiometry is certainly greater in the experiments of Ebel and Sack (1989, 1991) due to some slight Ag for Cu exchange with fahlore in the fahlore + electrum + pyrite + chalcopyrite assemblage. Despite the fact that the compositions of chalcopyrite were not determined in these experiments, we may reasonably conclude that the intercepts of $\bar{Q}_{X_4}^*$ at $X_3 = 0$ will decrease with increasing $X_{\text{Ag}}^{\text{ELEC}}$ due to the decreasing $a_{\text{CuFeS}_2}^{\text{CPY}}$ imposed by the condition of $\text{Ag}(\text{Cu})_{-1}$ exchange equilibrium for the chalcopyrite + pyrite + electrum subassemblage:



And this is indeed observed.

Despite the uncertainties in $\Delta\bar{G}_{\text{Ag}(\text{Cu})-1}^\circ$ consequent from our lack of knowledge of the exact compositions of chalcopyrite and its activity-composition relations, we may still tightly constrain $\Delta\bar{G}_{34}^\circ$ for a given assumed $\Delta\bar{G}_{3s}^*$ by evaluating the slope of $\bar{Q}_{X_4}^*$ with respect to X_3 at a given $X_{\text{Ag}}^{\text{ELEC}}$. Taking the average of values of $\Delta\bar{G}_{34}^\circ$

determined from the tightest reversal brackets of Ebel and Sack (1989, 1991) for $X_{\text{Ag}}^{\text{ELEC}}$ of 0.20 and 0.30 at 400°C and $X_{\text{Ag}}^{\text{ELEC}}$ of 0.30 and 0.40 at 300°C, we obtain the highly constrained functional dependence between $\Delta\bar{G}_{34}^{\circ}$ and $\Delta\bar{G}_{35}^*$ illustrated in Fig. 6, where it is apparent that the standard errors of the estimate of $\Delta\bar{G}_{34}^{\circ}$ decrease with decreasing $\Delta\bar{G}_{35}^*$. And utilizing values of $\Delta\bar{G}_{34}^{\circ}$ deduced for a given $\Delta\bar{G}_{35}^*$, we might derive the functional dependence of $RT \ln(a_{\text{CuFeS}_2}^{\text{CPY}})$ on $X_{\text{Ag}}^{\text{ELEC}}$ in the pyrite+electrum+chalcopyrite+fahlore assemblage from Eq. (26), information that would be useful in establishing activity–composition relations for chalcopyrite, if chalcopyrite compositions were known.

With the relationship between $\Delta\bar{G}_{34}^{\circ}$ and $\Delta\bar{G}_{35}^*$ established above, we may now consider what effects variations in $\Delta\bar{G}_{35}^*$ have on the topologies of miscibility gaps on the $(\text{Cu},\text{Ag})_{10}(\text{Fe},\text{Zn})_2\text{As}_4\text{S}_{13}$ back face and in the interior of the $(\text{Cu},\text{Ag})_{10}(\text{Fe},\text{Zn})_2(\text{Sb},\text{As})_4\text{S}_{13}$ fahlore cube. And, as noted above, positive values of $\Delta\bar{G}_{35}^*$ will move the miscibility gaps to lower values of X_4^{FAH} , and decreasing $\Delta\bar{G}_{35}^*$ has the opposite effect on miscibility gaps, as illustrated by Figs. 7 and 8 for the arsenic back face of the fahlore cube. It may be noted that the miscibility gaps for fahlores coexisting with sphalerite with a given $X_{\text{FeS}}^{\text{Sph}}$ are moved closer in X_4 to those for Fe-fahlores than those displayed on the Sb front face (Fig. 2) due to the incompatibility between As and Zn, an incompatibility which decreases the Zn content of fahlore due to increased Fe–Zn partitioning between fahlore and sphalerite. This movement is most extreme in the gaps for $\Delta\bar{G}_{35}^* = -10$ kJ/gfw on the right-hand-side (high X_4^{FAH}) of Fig. 7, where the gap for As-fahlores in Fe–Zn exchange equilibrium with sphalerite with $X_{\text{FeS}}^{\text{Sph}} = 0.01$ is nearly coincident with that for Fe-fahlore as consequence of the operation of both the incompatibilities between As and Zn, and of Ag and Zn in the fahlore structure. In addition, the critical temperatures of the As-fahlore miscibility gaps are only slightly lower than those determined for Sb-fahlores miscibility gaps (compare Figs. 2, 3), and, the critical temperature of the Zn-, As-fahlore miscibility gap declines relative to that for the Fe-, As-fahlore with increasing $\Delta\bar{G}_{35}^*$, with the result that it is at higher temperature with $\Delta\bar{G}_{35}^* = -10$ kJ/gfw, but at a lower temperature with $\Delta\bar{G}_{35}^* = +10$ kJ/gfw (compare Figs. 7, 8).

Variations in $\Delta\bar{G}_{35}^*$ have a much more significant effect on critical temperatures in the interior of the

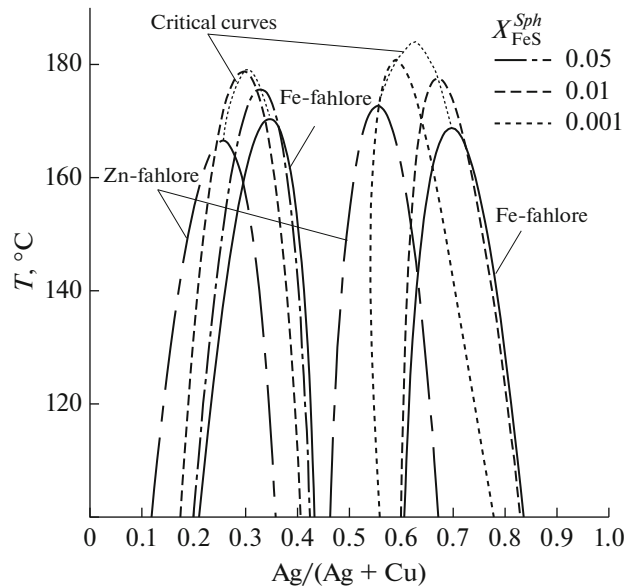


Fig. 7. Temperature–Ag/(Ag+Cu) relations of miscibility gaps in $(\text{Cu},\text{Ag})_{10}\text{Fe}_2\text{As}_4\text{S}_{13}$, $(\text{Cu},\text{Ag})_{10}\text{Zn}_2\text{As}_4\text{S}_{13}$, and $(\text{Cu},\text{Ag})_{10}(\text{Fe},\text{Zn})_2\text{As}_4\text{S}_{13}$ fahlores in Fe–Zn exchange equilibrium with sphalerites with $X_{\text{FeS}}^{\text{Sph}} = 0.001, 0.01,$ and 0.05 calculated for the assumptions that $\Delta\bar{G}_{35}^* = 10$ kJ/gfw (LHS) and -10 kJ/gfw (RHS). Dashed curves are the respective critical curves for these gap sets.

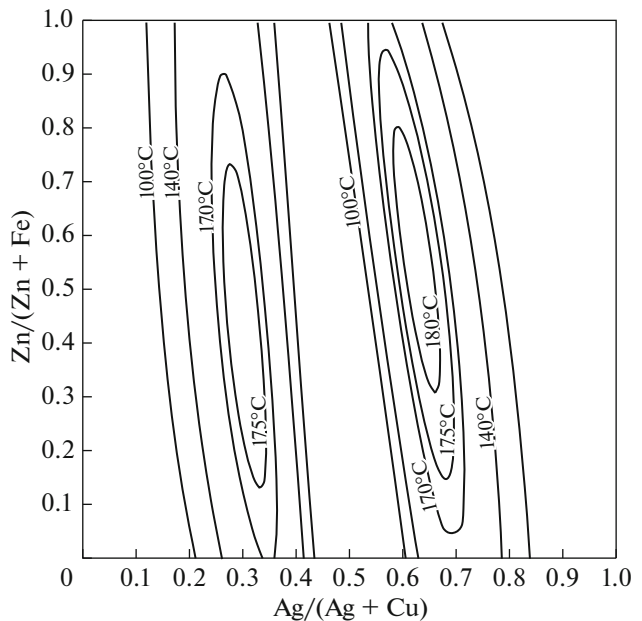


Fig. 8. Calculated 100, 140, 170, 175, and 180°C miscibility gaps for $(\text{Cu},\text{Ag})_{10}(\text{Fe},\text{Zn})_2\text{As}_4\text{S}_{13}$ fahlores using values of the parameter $\Delta\bar{G}_{35}^* = 10$ kJ/gfw (LHS) and $\Delta\bar{G}_{35}^* = -10$ kJ/gfw (RHS), values of $\Delta\bar{G}_{34}^{\circ}$ given by Fig. 6, and remaining parameter values from Table 1.

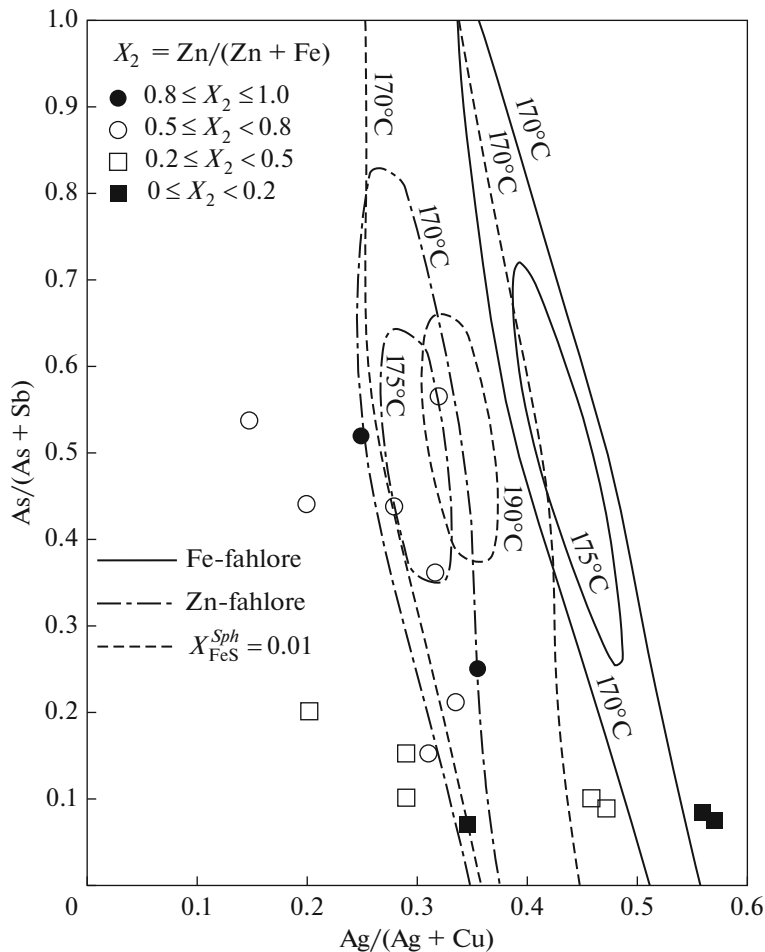


Fig. 9. Calculated 170, 175, and 190°C miscibility gaps for $(\text{Cu,Ag})_{10}(\text{Fe,Zn})_2(\text{Sb,As})_4\text{S}_{13}$ fahlores using $\Delta\bar{G}_{35}^* = 10$ kJ/gfw, the corresponding value of $\Delta\bar{G}_{34}^{\circ}$ given by Fig. 6, and remaining parameter values from Table 1. Circles and squares are a subset of the fahlores showing greatest departure from the $\text{Cu}_{10}(\text{Fe,Zn})_2(\text{Sb,As})_4\text{S}_{13}$ and $(\text{Cu,Ag})_{10}(\text{Fe,Zn})_2\text{Sb}_4\text{S}_{13}$ planes of the fahlore cube from the compilations of Sack et al. (1987), Sack (1992), and Sack and Ebel (1993).

fahlore cube. For the most positive value of $\Delta\bar{G}_{35}^*$ considered in Fig. 6, 10 kJ/gfw, the incompatibility between As and Ag, expressed by the parameter $\Delta\bar{G}_{34}^{\circ}$, is sufficiently small that there is minimal increase in critical temperatures relative to those on the front and back faces of the fahlore cube (compare Fig. 9), with maximum critical temperatures being less than 200°C, over 60°C below the corresponding critical temperatures, when it is assumed that $\Delta\bar{G}_{35}^* = 0$ kJ/gfw (compare Fig. 4). And, it is noteworthy that these adjustments leave the Ag-poor binodes of zincian fahlores virtually unmoved in $\text{Ag}/(\text{Ag}+\text{Cu})$ or X_4 at intermediate $\text{As}/(\text{As}+\text{Sb})$ and 170°C. The main effect of decreasing $\Delta\bar{G}_{35}^*$ (with the concomitant increase in $\Delta\bar{G}_{34}^{\circ}$) is to fill up the void in composition space not occupied by natural fahlores with miscibility gaps by increasing the $\text{Ag}/(\text{Ag}+\text{Cu})$ of their Ag-rich binodes.

And, for example, an adjustment of $\Delta\bar{G}_{35}^*$ to -10 kJ/gfw results in movement of the 170°C Ag-rich binode for the $(\text{Cu,Ag})_{10}(\text{Fe,Zn})_2(\text{Sb,As})_4\text{S}_{13}$ fahlore miscibility gaps for fahlores in Fe–Zn exchange equilibrium with sphalerites with $X_{\text{FeS}}^{\text{Sph}}$ of 0.01 and 0.07 to slightly higher $\text{Ag}/(\text{Ag}+\text{Cu})$ than the most Ag-rich fahlores of intermediate $\text{As}/(\text{As}+\text{Sb})$ ($X_4^{\text{FAH}} \approx 0.8$) reported by Ixer and Stanley (1983) (compare Fig. 10). The fahlores in the ores examined by Ixer and Stanley (1983) should be considered in more detail as they constitute a large percentage of the fahlore analyses exhibiting maximum departure from the $(\text{Cu,Ag})_{10}(\text{Fe,Zn})_2\text{Sb}_4\text{S}_{13}$ and $\text{Cu}_{10}(\text{Fe,Zn})_2(\text{Sb,As})_4\text{S}_{13}$ faces of the fahlore cube considered by Sack et al. (1987), Sack (1992) and Sack and Ebel (1993).

The fahlores described by Ixer and Stanley (1983) are from the Ag–Pb lode of the Hope mine on little

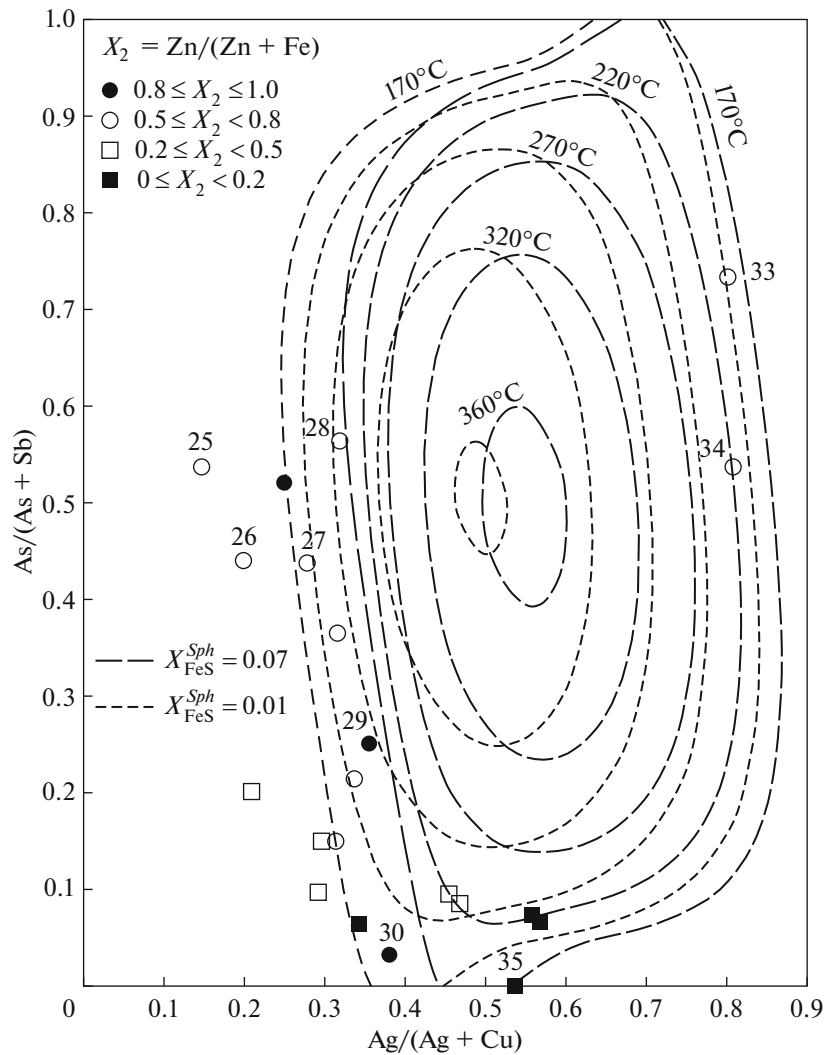
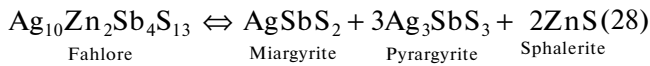


Fig. 10. Calculated 170, 220, 270, 320 and 360°C miscibility gaps for $(\text{Cu,Ag})_{10}(\text{Fe,Zn})_2(\text{Sb,As})_4\text{S}_{13}$ fahlores in Fe–Zn exchange equilibrium with $(\text{Zn,Fe})\text{S}$ sphalerites with $X_{\text{FeS}}^{\text{Sph}}$ of 0.01 and 0.07 for parameter values given in Table 1 with $\Delta\bar{G}_{3s}^* = -10$ and $\Delta\bar{G}_{34}^{\circ} = 61.817$ kJ/gfw. Circles and squares are fahlores showing greatest departure from the $\text{Cu}_{10}(\text{Fe,Zn})_2(\text{Sb,As})_4\text{S}_{13}$ and $(\text{Cu,Ag})_{10}(\text{Fe,Zn})_2\text{Sb}_4\text{S}_{13}$ planes of the fahlore cube from the compilations of Sack et al. (1987), Sack (1992), and Sack and Ebel (1993). Circles and squares with numbers are from Ixer and Stanley (1983), Table 1.

Sark Island, Channel Islands, Great Britain, the only mine that produced significant metalliferous ore in the Channel Islands in the nineteenth century. They occur in “Sark’s Hope Silver-Lead Lode” vein which cuts a foliated hornblende granite of Late Precambrian age. As is typical of such deposits, the paragenetic sequence for the minerals in Sark’s Hope lode is complicated, involving the minerals quartz, calcite, pyrite, hematite, chalcopryrite, bravoite, pyrrhotite, marcasite, arsenopyrite, fahlore, sphalerite, enargite, polybasite-pearceite, pyrargyrite, acanthite, galena, chalcocite, covellite and blaubleibender covellite (Ixer and Stanley, 1983). The fahlores of interest here (contain-

ing > 10 wt percent Ag; compare Fig. 10) occur as inclusions in both chalcopryrite and galena. Of particular interest is an inclusion of fahlore in chalcopryrite (analysis 30, Ixer and Stanley, 1983) with $X_2^{\text{FAH}} \approx 0.813$, $X_3^{\text{FAH}} \approx 0.0376$, and $X_4^{\text{FAH}} \approx 0.385$ in ores with sphalerites with $X_{\text{FeS}}^{\text{Sph}} \approx 0.016$ – 0.070 . This fahlore lies close enough to the $(\text{Cu,Ag})_{10}(\text{Fe,Zn})_2\text{Sb}_4\text{S}_{13}$ face of the fahlore cube that it may be used to place a minimum bound on mineralization temperature, if we assume it has not undergone significant retrograde Ag–Cu exchange with the chalcopryrite that encloses it. This minimum bound is in the range 240–250°C

based on the calibration of the condition of equilibrium for the reaction



of Sack (2005) and Sack and Lichtner (2009, 2010), and the absence of miargyrite in the ore specimens. One may, however, arrive at the conclusion that this minimum bound is not far below the actual mineralization temperature, if it is believed that galenas initially had higher Ag-contents, and much higher AgSbS_2 activities, during mineralization (for example, Sack and Goodell, 2002; Sack et al., 2003; Sack and Lichtner, 2009, 2010) than their current compositions indicate.

With this bound we may infer that the fahlores that occur as inclusions in galena which are Ag- and As-rich (analyses 33 and 34) are comfortably outside the binode of the miscibility gap for Ag-rich and Zn-rich fahlores at $\Delta\bar{G}_{3s}^* = -10$ kJ/gfw. We may also infer that the high Ag and As copper fahlores that occur as inclusions in chalcopyrite (analyses 28 and 29) are roughly equidistant in X_4^{FAH} from the corresponding binodes of such miscibility gaps for Ag-poor and Zn-rich fahlores. We may advance this coincidence as evidence that a value of $\Delta\bar{G}_{3s}^* = -10$ kJ/gfw is not a bad guess for its actual value. Of course, this requires us to assume that either As stabilizes high Ag-fahlores, or, as much more likely, the high-Ag fahlore inclusions in galena, like those in the interior and within the $(\text{Cu,Ag})_{10}(\text{Fe,Zn})_2\text{As}_4\text{S}_{13}$ face of the fahlore cube, may be metastable with respect to assemblages produced by reactions such as reaction (28), those involving argentite (for example, Ebel and Sack, 1991), arsenopyrite or other Ag- and As-rich sulfosalts. We thus conclude that these data of Ixer and Stanley support the inference that $\Delta\bar{G}_{3s}^*$ may be approximately -10 kJ/gfw. Not only would this topology provide a convenient explanation for the absence of fahlore compositions with intermediate Ag/(Ag+Cu) and As/(As+Sb) ratios, the inferred value of $\Delta\bar{G}_{3s}^*$ would comport well with the structural role for Ag in arsenian fahlores inferred by Johnson and Burnham (1985) and the observation that such values of $\Delta\bar{G}_{3s}^*$ lead to smaller standard errors in the estimate for $\Delta\bar{G}_{34}^\circ$ deduced from the tight experimental brackets of Ebel and Sack (1989, 1991). In addition, it is similar to the value determined for $\Delta\bar{G}_{4s}^*$ (compare Fig. 6). Of course such estimates for $\Delta\bar{G}_{3s}^*$ lead to greater critical temperatures, temperatures approaching 370°C.

DISCUSSION

We have presented a series of possible topologies of miscibility gaps in the $(\text{Cu,Ag})_{10}(\text{Fe,Zn})_2(\text{Sb,As})_4\text{S}_{13}$ fahlore cube for the purpose of helping to evaluate

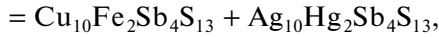
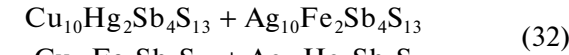
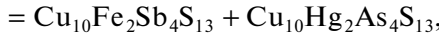
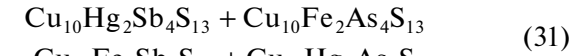
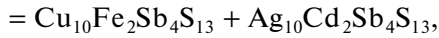
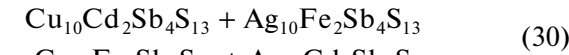
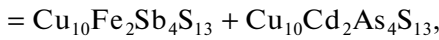
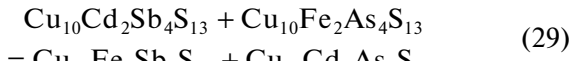
interpretations of the distribution of natural fahlore compositions, and, in the hope that they may encourage economic petrologists to find further direct, or indirect, evidence for them. To date, it has been 30 years since $(\text{Cu,Ag})_{10}(\text{Fe,Zn})_2\text{Sb}_4\text{S}_{13}$ fahlore miscibility gaps were predicted (O'Leary and Sack, 1987) and independently confirmed (Sack et al., 2003; Chinchilla et al., 2016). Accordingly, we have undertaken this analysis with the hope of catalyzing discovery of miscibility gaps in $(\text{Cu,Ag})_{10}(\text{Fe,Zn})_2(\text{Sb,As})_4\text{S}_{13}$ fahlores. And, as we previously noted, these gaps almost certainly extend to higher temperatures, and, are thus more extensive than those for $(\text{Cu,Ag})_{10}(\text{Fe,Zn})_2\text{Sb}_4\text{S}_{13}$ fahlores. Developing new constraints on miscibility gaps for arsenian fahlores will help refine out knowledge of the Gibbs energy surface of this remarkable petrogenetic indicator.

Our knowledge of the thermodynamic properties of this petrogenetic indicator is also hampered by the lack of a field tested estimate for \bar{G}_3° . This is the last unknown thermodynamic parameter, as the Gibbs energies of the $\text{Cu}_{10}\text{Zn}_2\text{As}_4\text{S}_{13}$, $\text{Ag}_{10}\text{Fe}_2\text{As}_4\text{S}_{13}$, and $\text{Ag}_{10}\text{Zn}_2\text{As}_4\text{S}_{13}$ vertices are related to it through Eqs. (1), (3), and (24), and field tested estimates for the Gibbs energies of $\text{Cu}_{10}\text{Fe}_2\text{Sb}_4\text{S}_{13}$ (\bar{G}_1°), $\text{Cu}_{10}\text{Zn}_2\text{Sb}_4\text{S}_{13}$ (\bar{G}_2°), $\text{Ag}_{10}\text{Fe}_2\text{Sb}_4\text{S}_{13}$ (\bar{G}_4°), and $\text{Ag}_{10}\text{Zn}_2\text{Sb}_4\text{S}_{13}$ ($\Delta\bar{G}_{24}^\circ - \bar{G}_1^\circ + \bar{G}_2^\circ + \bar{G}_4^\circ$) fahlores have been developed (Table 2; Sack and Lichtner, 2009, 2010). To be credible, any estimate of \bar{G}_3° must pass the rigorous field tests posed by metal zoning of arsenian fahlores in time and space (for example, Wu and Petersen, 1977) interpreted through the prism of state-of-the-art models for the thermodynamic properties of hydrothermal fluids (for example, Johnson et al., 1992; Shock et al., 1998; Reed and Palandri, 2006), reactive transport (for example, Lichtner, 1985; Lichtner et al., 1986a, 1986b, 1987; Lu and Lichtner, 2007; Hammond et al., 2008; Mills et al., 2009), and mineral kinetics (for example, Lichtner, 2016). It is with this aim that we intend to conduct inverse calculations to simulate such zoning and develop field tested constraints on \bar{G}_3° .

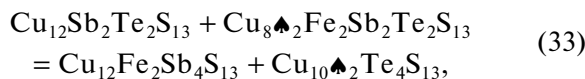
In these endeavors we must also develop a reliable model for the thermodynamic mixing properties of chalcopyrite solid solutions with Ag and Fe substituting for Cu to adequately constrain $\Delta\bar{G}_{\text{Ag}(\text{Cu})-1}^\circ$ in Eq. (26) and develop calibrations for hydrothermal fluid-sulfide equilibria that correctly describe ore-forming processes and events for this and other sulfide solid solutions, which, like chalcopyrite, do not retain their primary hydrothermal compositions (for example, galena, Sack et al., 2002, 2003, 2005; Sack and Goodell, 2002; Sack and Lichtner, 2009, 2010). With such improvements in our thermochemical models and parallel developments in kinetic theory (for example, Lichtner, 2016) we may begin to realize more of the true

potential of fahlore to serve as a powerful petrogenetic indicator of ore-forming process and events.

In addition, the energetics of the many substitutions which extend fahlore compositions beyond the $(\text{Cu,Ag})_{10}(\text{Fe,Zn})_2(\text{Sb,As})_4\text{S}_{13}$ cube (for example, $\text{Fe} \leftrightarrow \text{Mn}$, $\text{Fe} \leftrightarrow \text{Cd}$, $\text{Fe} \leftrightarrow \text{Hg}$, $\text{S} \leftrightarrow \text{Se}$, $2\text{Fe} \leftrightarrow \text{CuFe}^{3+}$, $\text{FeSb} \leftrightarrow \text{CuTe}$, and $\text{CuSb} \leftrightarrow \text{Te}$) need to be characterized to enable fahlore to tell us much more, perhaps nearly everything we need to know, about ore-forming processes and events. Fortunately this characterization may be aided by similarities between $(\text{Cu,Ag})_{10}(\text{Fe,Zn})_2(\text{Sb,As})_4\text{S}_{13}$ fahlores and those in more complex or parallel composition spaces. We may, for example, infer that the energies of the reciprocal reactions in which Zn is replaced by other group 12 elements Cd and Hg:



will be similar to those of reactions (1) and (2) (for example, Kalbskof, 1971; Patrick and Hall, 1983; Johnson and Rimstidt, 1986; Charnock et al., 1989). We may also note that the $2\text{Fe}^{2+} \leftrightarrow \text{CuFe}^{3+}$ substitution may be nearly ideal in synthetic $\text{Cu}_{10}\text{Fe}_2\text{Sb}_4\text{S}_{13}$ - $\text{Cu}_{11}\text{FeSb}_4\text{S}_{13}$ fahlores (for example, Makovicky et al., 1990), but the operation of the $\text{Fe} \leftrightarrow \text{Zn}$ substitution may complicate phase relations in such fahlores even at 220°C (for example, Sack and Goodell, 2002, Fig. 5). In addition, we might be tempted to surmise that there is an incompatibility between vacancies (\blacklozenge) in trigonal-planar coordination and Fe^{2+} in tetrahedral coordination in Te-substituted fahlores, expressed by a large negative value for the Gibbs energy of the reciprocal reaction:



because many natural Te-fahlore (that is, goldfieldite) occurrences tend to lie close to the $(\text{Cu,Ag})_{10}(\text{Fe,Zn})_2(\text{Sb,As})_4\text{S}_{13}$ - $(\text{Cu,Ag})_{12}(\text{Sb,As})_2\text{Te}_2\text{S}_{13}$ and $(\text{Cu,Ag})_{12}(\text{Sb,As})_2\text{Te}_2\text{S}_{13}$ - $(\text{Cu,Ag})_{10}\blacklozenge_2\text{Te}_4\text{S}_{13}$ pseudobinaries (for example, Kalbskof, 1974; Kase, 1986; Shimizu and Stanley, 1991; Trudu and Knittel, 1998; Plotinskaya et al., 2005a, 2005b). However, the presence of Te-fahlores with $(\text{Fe} + \text{Zn}) \approx 2$ and $\text{Te} \approx 2$ (for example, Kovalenker et al., 1980; Trudu and Knittel, 1998, Fig. 8) suggests that, rather than the Gibbs energy of $\text{Cu}_8\blacklozenge_2\text{Fe}_2\text{Sb}_2\text{Te}_2\text{S}_{13}$ being significantly greater than that defined by the plane containing the

Table 2. Enthalpies and entropies of formation of $(\text{Cu,Ag})_{10}(\text{Fe,Zn})_2\text{Sb}_4\text{S}_{13}$ fahlore endmembers and FeS sphalerite from simple sulfides at 1 bar and between 177 and 435°C (from Sack and Lichtner, 2009, 2010)¹

Mineral	$\Delta\bar{H}_f$, kJ/gfw	$\Delta\bar{S}_f$, J/K-gfw
$\text{Cu}_{10}\text{Fe}_2\text{Sb}_4\text{S}_{13}^2$	-140.2561	0.565
$\text{Cu}_{10}\text{Fe}_2\text{Sb}_4\text{S}_{13}^3$	-139.461	1.894
$\text{Cu}_{10}\text{Zn}_2\text{Sb}_4\text{S}_{13}$	-120.8817	8.309
$\text{Ag}_{10}\text{Fe}_2\text{Sb}_4\text{S}_{13}^2$	-47.6869	0.621
$\text{Ag}_{10}\text{Fe}_2\text{Sb}_4\text{S}_{13}^3$	-46.8919	1.950
$\text{Ag}_{10}\text{Zn}_2\text{Sb}_4\text{S}_{13}$	-19.3124	8.365
FeS ²	-1.0188	-3.872
FeS ³	-0.6213	-3.207

¹ Between 177 and 435°C the reference simple sulfides are bcc- Ag_2S , hcp- Cu_2S , ZnS sphalerite, FeS troilite, and Sb_2S_3 stibnite.

Values for $\Delta\bar{G}_1^\circ$, $\Delta\bar{G}_2^\circ$, and $\Delta\bar{G}_3^\circ$ were field tested. That is to say these values lead to predicted fluids compositions that are consistent with observations from the Coeur d'Alene and Keno Hill mining districts (for example, Sack et al., 2002, 2003, 2005): we inferred primary mineral compositions from petrologic data, mass balance, salinity, CO_2 contents and temperature constraints from fluid inclusions, and from phase equilibrium considerations, and then demonstrated that the calculated fluids were in equilibrium with the inferred primary assemblages (Sack and Lichtner, 2009, 2010); ² $T > 324.85^\circ\text{C}$.; ³ 324.85 – 177°C , temperature of bcc- Ag_2S transition to acanthite.

Gibbs energies of the $\text{Cu}_{10}\text{Fe}_2\text{Sb}_4\text{S}_{13}$, $\text{Cu}_{12}\text{Sb}_2\text{Te}_2\text{S}_{13}$ and $\text{Cu}_{10}\blacklozenge_2\text{Te}_4\text{S}_{13}$ endmember components, the close conformity between many natural Te-fahlore compositions and these pseudobinaries may reflect that lower $\blacklozenge\text{Te}(\text{CuSb})_{-1}$ and/or higher $\text{CuTe}(\text{FeSb})_{-1}$ exchange potentials prevailed in the main, than in the rare cases where fahlores near the $(\text{Cu,Ag})_{10}(\text{Fe,Zn})_2(\text{Sb,As})_4\text{S}_{13}$ - $(\text{Cu,Ag})_8\blacklozenge_2(\text{Fe,Zn})_2\text{Te}_2(\text{Sb,As})_2\text{S}_{13}$ and $(\text{Cu,Ag})_8\blacklozenge_2(\text{Fe,Zn})_2\text{Te}_2(\text{Sb,As})_2\text{S}_{13}$ – $(\text{Cu,Ag})_{12}\text{Te}_2(\text{Sb,As})_2\text{S}_{13}$ pseudobinaries were produced (compare Trudu and Knittel, 1998, Fig. 8). Thus, the exact energy of reaction (33) is subject to large uncertainty, and it, like many other energetic parameters of fahlores in composition spaces extending beyond the fahlore cube, are not well characterized, and thus provide fertile grounds for further study.

Finally, analysis of the energetic properties of Te-bearing fahlores may be further complicated by the operation of the Cu^{2+} for Fe^{2+} substitution in Te-poor varieties. Although natural fahlores typically have Cu^{2+} much less than 10 percent of the divalent cations (for example, Tatsuka and Morimota, 1977b; Johnson and Jeanloz, 1983) many of the Te-poor fahlores reported by Shimizu and Stanley (1991), Trudu and Knittel (1998), and Plotinskaya et al. (2005a, 2005b) have greater Cu^{2+} substituting for Fe^{2+} and/or $\text{Cu}^+\text{Fe}^{3+}$ substituting for 2Fe^{2+} (for example, Makovicky et al., 1990). And additional removal of Fe from

synthetic tetrahedrites in the Cu-Fe-Sb-S system further complicates matters by expanding tetrahedrite's stability field from virtually a point for $\text{Cu}_{10}\text{Fe}_2\text{Sb}_4\text{S}_{13}$ fahlore, our stoichiometric basis component, to a roughly triangular composition field with one vertex approaching $\text{Cu}_{14}\text{Sb}_4\text{S}_{13}$ and the other two vertices lying roughly 85 and 60 percent towards the compositions $\text{Cu}_{12}\text{Sb}_4\text{S}_{13}$ and $\text{Cu}_{12}\text{Sb}_{4.67}\text{S}_{13}$ along the joins $\text{Cu}_{14}\text{Sb}_4\text{S}_{13}$ - $\text{Cu}_{12}\text{Sb}_4\text{S}_{13}$ and $\text{Cu}_{14}\text{Sb}_4\text{S}_{13}$ - $\text{Cu}_{12}\text{Sb}_{4.67}\text{S}_{13}$ in the system Cu-Sb-S at 500°C (for example, Tatsuka and Morimoto, 1977a; Makovicky and Skinner, 1978). With decreasing temperatures, such non-stoichiometric Cu-Sb-S tetrahedrites become unstable or metastable with respect to other sulfides, as well as to unmixing into tetrahedrites approaching 204 and 208 valence electrons per unit cell, coexisting tetrahedrites with full or near full occupancy of the 51st and 52nd Brillouin zones, respectively (for example, Makovicky and Skinner, 1978, 1979; Johnson and Jeanloz, 1983). There appears to be little relationship between miscibility gaps in synthetic fahlores in such simple chemical systems and miscibility gaps in natural fahlores. Natural fahlores are invariably more chemically diverse, and adhere more closely to the 208 valence electrons per unit cell that corresponds to a full 52nd Brillouin zone that characterizes all fahlores of the fahlore cube. Miscibility gaps in the cube are a consequence of changing site preference of Ag with Ag/(Ag + Cu) ratio and substantial nonideality in the mixing of Ag and Cu on tetrahedral metal sites, and are enhanced by the incompatibility between Ag and As in fahlores with intermediate Ag/(Ag + Cu) and As/(As + Sb) ratios.

CONCLUSIONS

Possible topologies of miscibility gaps in $(\text{Cu},\text{Ag})_{10}(\text{Fe},\text{Zn})_2(\text{Sb},\text{As})_4\text{S}_{13}$ fahlores, consistent with established phase relations for $(\text{Cu},\text{Ag})_{10}(\text{Fe},\text{Zn})_2\text{Sb}_4\text{S}_{13}$ fahlores, and experimental and natural constraints on the incompatibilities of As and Zn and of As and Ag in the fahlore structure, require that As stabilizes Ag in trigonal-planar metal sites relative to $(\text{Cu},\text{Ag})_{10}(\text{Fe},\text{Zn})_2\text{Sb}_4\text{S}_{13}$ fahlores to be consistent with the distribution of natural fahlore compositions. The resulting thermochemical model for fahlores predicts that miscibility gaps for $(\text{Cu},\text{Ag})_{10}(\text{Fe},\text{Zn})_2\text{As}_4\text{S}_{13}$ fahlores are displaced to higher Ag/(Ag+Cu) ratios than their $(\text{Cu},\text{Ag})_{10}(\text{Fe},\text{Zn})_2\text{Sb}_4\text{S}_{13}$ counterparts, but have similar critical temperatures in the range of 170–185°C. In contrast, we infer these gaps extend to temperatures exceeding 360°C in $(\text{Cu},\text{Ag})_{10}(\text{Fe},\text{Zn})_2(\text{Sb},\text{As})_4\text{S}_{13}$ fahlores. Activity—composition relations are now well calibrated for all of the vertices of the $(\text{Cu},\text{Ag})_{10}(\text{Fe},\text{Zn})_2(\text{Sb},\text{As})_4\text{S}_{13}$ fahlore cube, the Gibbs energies of formation of $(\text{Cu},\text{Ag})_{10}(\text{Fe},\text{Zn})_2\text{Sb}_4\text{S}_{13}$ fahlore endmembers have been calibrated and field tested, and the Gibbs energies of formation of only one

$(\text{Cu},\text{Ag})_{10}(\text{Fe},\text{Zn})_2\text{As}_4\text{S}_{13}$ fahlore endmember needs to be calibrated and field tested to complete the fahlore thermochemical model. With this development the fahlore thermochemical model may be used to make predictions about metal zoning in time and space, with the ultimate goal of developing strategies of mineral exploration and resource evaluation based on sound thermodynamic, kinetic and reactive transport models.

ACKNOWLEDGMENTS

This paper is dedicated to the memories of Dimitrii S. Korzhinskii and James B. Thompson, Jr., whose collaboration fundamentally changed our understanding of the thermodynamics of open systems, and to those of Steven Ensign Bushnell and O'Win (Winney) Sack. I acknowledge JBT for his many contributions to my professional and personal development, Steve for being such a good friend and introducing me to fahlore thermochemistry by asking the right questions, helpful discussions with, and reviews from, Peter Lichtner and Lisa Hardy, and the helpful and thought provoking critiques and suggestions of Attila Kilinc and Olga Plotinskaya. Finally I thank Leonya Aranovich and Nikolay Bortnikov for arranging my visit to IGEM and stimulating discussions, and acknowledge the support of the OFM Research Corporation and its friendly staff: Odee, Filo, Milo and recently deceased O'Win Sack, a formerly AA rated racing greyhound who raced her way into my heart.

REFERENCES

- Balabin, A.I. and Sack, R.O., Thermodynamics of (Zn, Fe)S sphalerite: a CVM approach with large basis clusters, *Mineral. Mag.*, 2000, vol. 64, pp. 923–943.
- Breslovskaya, V. and Tarkian, M., Compositional variation in Bi-bearing fahlores, *Neues Jahrb. Mineral., Monatsh.*, 1994, vol. 1994, pp. 230–240.
- Bushnell, S.E., Paragenesis and Zoning of the Cananea–Duluth breccia pipe, Sonora, Mexico: *Ph. D. Thesis*, Cambridge, Massachusetts: Harvard University, 1983.
- Cabri, L.J., New data on phase relations in the Cu–Fe–S system, *Econ. Geol.*, 1973, vol. 68, pp. 443–454.
- Charlat, M. and Levy, C., Substitutions multiples dans la serie tennantite-tetrahedrite, *Bull. Soc. Fr. Mineral. Petrol.*, 1974, vol. 97, pp. 241–250.
- Charlat, M. and Levy, C., Influence principales sue le parametre cristallin dans la serie tennantite-tetrahedrite, *Bull. Soc. Fr. Mineral. Petrol.*, 1975, vol. 97, pp. 241–250.
- Charnock, J.M., Garner, C.D., Patrick, R.A.D., and Vaughan, D.J., Investigation into the nature of copper and silver sites in Argentinian tetrahedrite using EXAFS spectroscopy, *Phys. Chem. Mineral.*, 1988, vol. 15, pp. 296–299.
- Charnock, J.M., Garner, C.D., Patrick, R.A.D., and Vaughan, D.J., Coordination sites of metals in tetrahedrite minerals determined by EXAFS, *J. Solid State Chem.*, 1989, vol. 82, pp. 279–289.

- Chinchilla, D., Ortega, L., Piña, R., et al., The Patricia Zn–Pb–Ag epithermal ore deposit: an uncommon type of mineralization in northeastern Chile, *Ore Geol. Rev.*, 2016, vol. 73, pp. 104–126.
- Chutas, N.I. and Sack, R.O., Ore genesis at La Colorada Ag–Zn–Pb deposit in Zacatecas, Mexico, *Mineral. Mag.*, 2004, vol. 68, no. 6, pp. 923–937.
- Chutas, N.I., Kress, V.C., Ghiorso, M.S., and Sack, R.O., A solution model for high-temperature PbS–AgSbS₂–AgBiS₂ galena, *Am. Mineral.*, 2008, vol. 93, pp. 1630–1640.
- Cronstedt, A.F., *Försök til Mineralogie, Eller Mineral-Rikets Upställning*, Stockholm, Wilde, 1758
- Ebel, D.S. and Sack, R.O., Ag–Cu and As–Sb exchange energies in tetrahedrite–tennantite fahlores, *Geochim. Cosmochim. Acta*, 1989, vol. 53, pp. 2301–2309.
- Ebel, D.S. and Sack, R.O., As–Ag incompatibility in fahlores, *Mineral. Mag.*, 1991, vol. 55, pp. 521–528.
- Engi, M., Equilibria involving Al–Cr spinel: Mg–Fe exchange with olivine. experiments, thermodynamic analysis, and consequences of geothermometry, *Am. J. Sci.*, 1983, vol. 283A, pp. 29–71.
- Evans, B.W. and Frost, R.G., Chrome-spinel in progressive metamorphism—a preliminary analysis, *Geochim. Cosmochim. Acta*, 1975, vol. 39, pp. 959–972.
- Gaines, R.V., Skinner, H.C.W., Foord, E.E., et al., *Dana's New Mineralogy*, 8th ed, New York: John Wiley & Sons, 1997.
- Gamyranin, G.N., Bortnikov, N.S., Alpatov, V.V., et al., The Kupol'noe silver–tin deposit (Sakha Republic, Russia): an example of the evolution of an ore–magmatic system, *Geol. Ore Deposits*, 2001, vol. 43, no. 6, pp. 442–467.
- Ghiorso, M.S., The application of the Darken equation to mineral solid solutions with variable degrees of order–disorder, *Am. Mineral.*, 1990, vol. 104, pp. 539–543.
- Ghosal, S. and Sack, R.O., As–Sb energetics in Argentinian sulfosalts, *Geochim. Cosmochim. Acta*, 1995, vol. 59, pp. 3573–3579.
- Ghosal, S. and Sack, R.O., Bi–Sb energetics in sulfosalts and sulfides, *Mineral. Mag.*, 1999, vol. 63, pp. 723–733.
- Goodell, P.C., Zoning and Paragenesis in the Julcani District, Peru: a Study of Metal Ratios: *Ph. D. Thesis*, Cambridge: Massachusetts: Harvard University, 1970.
- Hall, A.J., Substitution of Cu by Zn, Fe and Ag in synthetic tetrahedrite, *Bull. Soc. Franc. Minéral. Petrol.*, 1972, vol. 95, pp. 583–594.
- Hammond, G.E., Lichtner, P.C., Mills, R.T., and Lu, C., Toward petascale computing in geosciences: application to the Hanford 300 Area, *J. Phys. Conference Ser.*, 2008, vol. 125, pp. 1–10; 012051. doi 10.1088/1742-6596/125/1/012051
- Harlov, D.E. and Sack, R.O., Thermochemistry of polybasite–pearceite solutions, *Geochim. Cosmochim. Acta*, 1994, vol. 58, pp. 4363–4375.
- Hernández, A.N.G. and Akasaka, M., Silver-bearing and associated minerals in El Zancudo deposit, Antioquia, Colombia, *Res. Geol.*, 2007, vol. 57, no. 4, pp. 386–399.
- Hernández, A.N.G. and Akasaka, M., Ag-rich tetrahedrite in the El Zancudo deposit, Colombia: occurrence, chemical compositions and genetic temperatures, *Res. Geol.*, 2010, vol. 60, no. 3, pp. 218–233.
- Ixer, R.A. and Stanley, C.J., Silver mineralization at Sark's Hope mine, Sark, Channel Islands, *Mineral. Mag.*, 1983, vol. 47, pp. 539–545.
- Johnson, M.L. and Burnham, C.W., Crystal structure refinement of an arsenic bearing Argentinian tetrahedrite, *Am. Mineral.*, 1985, vol. 70, pp. 165–170.
- Johnson, M.L. and Jeanloz, R.A., A Brillouin-zone model for compositional variation in tetrahedrite, *Am. Mineral.*, 1983, vol. 68, pp. 220–226.
- Johnson, N.E. and Rimstidt, J.D., Compositional trends in tetrahedrite, *Can. Mineral.*, 1986, vol. 24, pp. 385–397.
- Kalbskopf, R., Die koordination des quicksilbers im schwazit, *Tschermaks Mineralogie und Petrographie Mitteilungen*, 1971, vol. 18, pp. 173–175.
- Kalbskopf, R., Strukturverfeinerung des freibergs, *Tschermaks Mineralogie und Petrographie Mitteilungen*, 1972, vol. 19, pp. 147–155.
- Kalbskopf, R., Synthese und kristallstruktur von Cu_{12-x}Te₄S₁₃, dem tellur-endglied der fahlerze, *Tschermaks Mineralogie und Petrographie Mitteilungen*, 1974, vol. 21, pp. 147–155.
- Karop-Møller, S. and Makovicky, E., Exploratory studies of substitutions in tetrahedrite–tennantite solid solutions. Part V: mercurian tetrahedrite, *Neues Jahrb. Mineral. Abh.*, 2003, vol. 179, pp. 73–83.
- Kase, K., Tellurium tennantite from the Besshi-type deposits of the Sambagawa metamorphic belt, Japan, *Can. Mineral.*, 1986, vol. 24, pp. 399–404.
- Klünder-Hansen, M., Makovicky, E., and Karop-Møller, S., Exploratory studies of substitutions in tetrahedrite–tennantite solid solutions. Part IV. Substitution of germanium and tin, *Neues Jahrb. Mineral. Abh.*, 2003, vol. 179, pp. 43–71.
- Klünder-Hansen, M., Karop-Møller, S., and Makovicky, E., Exploratory studies of substitutions in tetrahedrite–tennantite solid solutions. Part III. The solubility of bismuth in tetrahedrite–tennantite containing iron and zinc, *Neues Jahrb. Mineral. Mitteil.*, 2003b, vol. 2003, pp. 153–175.
- Kovalenker, V.A., Troneva, N.V., and Dobronichenko, V.V., Unusual compositions of the main ore-forming minerals of the pipe-shaped ore deposit of Kochbulashk, *Methods for the Investigation of Ore-Forming Sulfides and their Paragenesis*, Moscow, 1980, pp. 140–164.
- Lichtner, P.C., Continuum model for simultaneous chemical reactions and mass transport in hydrothermal systems, *Geochim. Cosmochim. Acta*, 1985, vol. 49, pp. 779–800.
- Lichtner, P.C., Kinetic rate laws invariant to scaling the mineral formula unit, *Am. J. Sci.*, 2016, vol. 316, no. 5, pp. 437–469.
- Lichtner, P.C., Oelkers, E.H., and Helgeson, H.C., Exact and numerical solutions to the moving boundary problem resulting from reversible heterogeneous reactions and aqueous diffusion in a porous medium, *J. Geophys. Res.*, 1986a, vol. 91, pp. 7531–7544.
- Lichtner, P.C., Oelkers, E.H., and Helgeson, H.C., Interdiffusion with multiple precipitation/dissolution reactions, *Geochim. Cosmochim. Acta*, 1986b, vol. 50, pp. 1951–1966.
- Lichtner, P.C., Helgeson, H.C., and Murphy, W.M., *Lagrangian and eulerian representations of metasomatic alteration of minerals*, *Chemical Transport in Metasomatic Process*, Helgeson, H.C., Eds., Dordrecht: Reidel, 1987, 519–545.

- Lu, C. and Lichtner, P.C., High resolution numerical investigation on the effect of convective instability on long term CO₂ storage in saline aquifers, *J. Phys. Conf. Ser.*, 2007, vol. 78, pp. 1–6; 012042. doi 10.1088/1742-6596/78/1/012042
- Lynch, J.V.G., Large-scale hydrothermal zoning reflected in the tetrahedrite–freibergite solid solution, Keno Hill Ag–Pb–Zn district, Yukon, *Can. Mineral.*, 1989, vol. 27, pp. 383–400.
- Makovicky, E., Crystal structures of sulfides and other chalcogenides, *Sulfide Mineralogy and Geochemistry*, Vaughan, D.J., Ed., *Mineral. Soc. Amer. Rev. Mineral. Geochem.*, 2006, vol. 61, pp. 7–125.
- Makovicky, E. and Karop-Møller, S., Exploratory studies on substitution of minor elements in synthetic tetrahedrite. Part I: Substitution by Fe, Zn, Co, Ni, Mn, Cr, V, and Pb. Unit-cell parameter changes on substitution and the structural role of Cu²⁺, *Neues Jahrb. Mineral. Abh.*, 1994, vol. 167, pp. 89–123.
- Makovicky, E. and Skinner, B.J., Studies of the sulfosalts of copper VI. Low-temperature exsolution in synthetic tetrahedrite solid solution, Cu_{12+x}Sb₄ + yS₁₃, *Can. Mineral.*, 1978, vol. 16, pp. 611–623.
- Makovicky, E. and Skinner, B.J., Studies of the sulfosalts of copper VII. Crystal structures of the exsolution products Cu_{12.3}Sb₄S₁₃ and Cu_{13.8}Sb₄S₁₃, *Can. Mineral.*, 1979, vol. 17, pp. 619–634.
- Makovicky, E., Forcher, K., Lottermoser, W., and Amthauer, G., The role of Fe²⁺ and Fe³⁺ in synthetic Fe-substituted tetrahedrite, *Mineral. Petrol.*, 1990, vol. 43, pp. 73–81.
- Mills, R.T., Hammond, G.E., Lichtner, P.C., et al., Modeling subsurface reactive flows using leadership-class computing, *J. Phys. Conf. Ser.*, 2009, vol. 180, pp. 1–10; 012062. doi 10.1088/1742-6596/180/1/012062
- Mozgova, N.N. and Tsepin, A.I., *Grey Ores: Aspects of Chemical Composition and Properties*, Moscow: Nauka, 1983.
- O’Leary, M.J. and Sack, R.O., Fe–Zn exchange reaction between tetrahedrite and sphalerite in natural environments, *Contrib. Mineral. Petrol.*, 1987, vol. 96, pp. 415–425.
- Patrick, R.A.D. and Hall, A.J., Silver substitution into synthetic zinc, cadmium and iron tetrahedrites, *Mineral. Mag.*, 1983, vol. 47, pp. 441–445.
- Pauling, L. and Newmann, E.W., The crystal structure of binnite (Cu, Fe)₁₂As₄S₁₃ and the chemical composition of minerals of the tetrahedrite group, *Zeitsch. Kristall.*, 1934, vol. 88, pp. 54–62.
- Plotinskaya, O.Yu., Rusinov, V.L., Kovalenker, V.A., and Seltmann, R., Oscillatory zoning in goldfieldite as a possible indicator of their formation conditions, *Geochem. Mineral. Petrol.*, 2005a, vol. 43, pp. 142–147.
- Plotinskaya, O.Yu., Kovalenker, V.A., Rusinov, V.L., and Seltmann, R., Oscillatory zoning in goldfieldite from epithermal gold deposits, *Dokl. Earth Sci.*, 2005b, vol. 304, no. 5, pp. 799–802.
- Raabe, K.C. and Sack, R.O., Growth zoning in tetrahedrite from the hock hocking mine, *Can. Mineral.*, 1984, vol. 22, pp. 577–582.
- Reed, M.H. and Palandri, J., *SOLTHERM: Data Base of Equilibrium Constants for Aqueous-Mineral-Gas Equilibria*, University of Oregon, 2006.
- Ramdohr, P., *The Ore Minerals and their Intergrowths*, London: Pergamon, 1969.
- Ross, N.L. and Price, G.D., *The Stability of Minerals*, London: Chapman and Hall, 1992.
- Sack, R.O., Spinels as petrogenetic indicators: activity-composition relations at low pressures, *Contrib. Mineral. Petrol.*, 1982, vol. 79, pp. 169–182.
- Sack, R.O., Thermochemistry of tetrahedrite-tennantite fahlores, *The Stability of Minerals*, Ross, N.L., and Price, G.D., Eds., London, Chapman and Hall, 1992, pp. 243–266.
- Sack, R.O., Internally consistent database for sulfides and sulfosalts in the system Ag₂S–Cu₂S–ZnS–Sb₂S₃–As₂S₃, *Geochim. Cosmochim. Acta*, 2000, vol. 64, pp. 3803–3812.
- Sack, R.O., Note on “large-scale” hydrothermal zoning reflected in the tetrahedrite–freibergite solid solution, Keno Hill Ag–Pb–Zn district, “Yukon”, J.V. Gregory Lynch, Ed., *Can. Mineral.*, 2002, vol. 40, pp. 1717–1719.
- Sack, R.O., Internally consistent database for sulfides and sulfosalts in the system Ag₂S–Cu₂S–ZnS–FeS–Sb₂S₃–As₂S₃, *Geochim. Cosmochim. Acta*, 2005, vol. 69, pp. 1157–1164.
- Sack, R.O., MgAl₂O₄–Al_{8/3}O₄ spinels. Formulation and calibration of the low-pressure thermodynamics of mixing, *Am. J. Sci.*, 2014, vol. 314, no. 4, pp. 858–877.
- Sack, R.O. and Brackebusch, F., Fahlore as an indicator of mineralization temperature and gold fineness, *CIM Bull.*, 2004, vol. 97, pp. 78–83.
- Sack, R.O. and Ebel, D.S., As–Sb exchange energies in tetrahedrite-tennantite fahlores and bournonite-seligmannite solid solutions, *Mineral. Mag.*, 1993, vol. 57, pp. 635–642.
- Sack, R.O. and Ghiorso, M.S., An internally consistent model for the thermodynamic properties of Fe–Mg titanomagnetite–aluminates spinels, *Contrib. Mineral. Petrol.*, 1991a, vol. 106, pp. 474–505.
- Sack, R.O. and Ghiorso, M.S., Chromian spinels as petrogenetic indicators: thermodynamics and petrological applications, *Am. Mineral.*, 1991b, vol. 76, pp. 827–847.
- Sack, R.O. and Goodell, P.C., Retrograde reactions involving galena and Ag-sulfosalts in a zoned ore deposit, Julcani, Peru, *Mineral. Mag.*, 2002, vol. 66, pp. 1043–1062.
- Sack, R.O. and Lichtner, P.C., Constraining compositions of hydrothermal fluids in equilibrium with polymetallic ore-forming sulfide assemblages, *Econ. Geol.*, 2009, vol. 104, pp. 1249–1264.
- Sack, R.O. and Lichtner, P.C., *Econ. Geol.*, 2010, vol. 105, no. 1, p. 249. <http://dx.doi.org/10.2113/gsecongeo.105.1.249>
- Sack, R.O. and Loucks, R.R., Thermodynamic properties of tetrahedrite–tennantites. I. Constraints on the interdependencies of the Ag↔Cu, Fe↔Zn, Cu↔Fe, and As↔Sb exchange reactions, *Am. Mineral.*, 1985, vol. 70, pp. 1270–1289.
- Sack, R.O., Ebel, D.S., and O’Leary, M.J., *Tetrahedrite thermochemistry and metal zoning*, *Chemical Transport in Metasomatic Processes*, Helgeson, H.C., Ed., Dordrecht: Reidel, NATO Advanced Study Institute, 1987, pp. 701–731.
- Sack, R.O., Kuehner, S.M., and Hardy, L.S., Retrograde Ag-enrichment in fahlores from the Coeur d’Alene mining district, Idaho, USA, *Mineral. Mag.*, 2002, vol. 66, pp. 215–229.

- Sack, R.O., Lynch, J.G.V., and Foit, F.F., Fahlore as a petrogenetic indicator: Keno Hill Ag–Pb–Zn district, Yukon, Canada, *Mineral. Mag.*, 2003, vol. 67, pp. 1023–1038.
- Sack, R.O., Fredericks, R.M., Hardy, L.S., and Ebel, D.S., Origin of high-silver fahlores from the Galena mine, Wallace, Idaho, USA, *Am. Mineral.*, 2005, vol. 90, pp. 1000–1007.
- Shimizu, M. and Stanley, C.J., Coupled substitutions in goldfieldite–tetrahedrite minerals from the Ikiri mine, Japan, *Mineral. Mag.*, 1991, vol. 55, pp. 515–519.
- Shock, E.L., et al., SLOP98.dat (computer data file), 1998. <http://geopig.asu.edu/sites/default/files/slop98.dat>.
- Spiridonov, E.M., Species and varieties of fahlore (tetrahedrite–tennantite) and their rational nomenclature, *Dokl. Akad. Nauk SSSR*, 1984, vol. 279, pp. 166–172.
- Spiridonov, E.M. and Okrugin, V.M., Selenium goldfieldite, a new fahlore variety, *Dokl. Akad. Nauk SSSR*, 1985, vol. 280, pp. 476–478.
- Sugaki, A., Shima, H., Kitakaze, A., and Harada, H., Isothermal phase relations in the system Cu–Fe–S under hydrothermal conditions at 350°C and 300°C, *Econ. Geol.*, 1975, vol. 70, pp. 806–823.
- Tatsuka, K. and Morimoto, N., Tetrahedrite stability relations in the Cu–Sb–S system, *Econ. Geol.*, 1977a, vol. 72, pp. 258–270.
- Tatsuka, K. and Morimoto, N., Tetrahedrite stability relations in the Cu–Fe–Sb–S system, *Am. Mineral.*, 1977b, vol. 62, pp. 1101–1109.
- Thompson, J.B., Jr., Chemical reactions in crystals, *Am. Mineral.*, 1969, vol. 54, pp. 341–375.
- Thompson, J.B., Jr., Chemical reactions in crystals. Corrections and clarifications, *Am. Mineral.*, 1970, vol. 55, pp. 528–532.
- Trudu, A.G. and Knittel, U., Crystallography, mineral chemistry and chemical nomenclature of goldfieldite, the tellurian member of the tetrahedrite solid-solution series, *Can. Mineral.*, 1998, vol. 36, pp. 1115–1137.
- White, J.L., Orr, R.L., and Hultgreen, R., The thermodynamic properties of gold–silver alloys, *Acta Metall.*, 1957, vol. 5, pp. 747–760.
- Wu, I. and Petersen, U., Geochemistry of tetrahedrite–tennantite at Casapalca, Peru, *Econ. Geol.*, 1977, vol. 72, pp. 933–1016.
- Wuensch, B.J., The crystal structure of tetrahedrite, $\text{Cu}_{12}\text{Sb}_4\text{S}_{13}$, *Zeitschrift für Kristallographie*, 1964, vol. 119, pp. 437–453.
- Wuensch, B.J., Takeuchi, Y., and Nowack, W., Refinement of the crystal structure of binnite, $\text{Cu}_{12}\text{As}_4\text{S}_{13}$, *Zeitschrift für Kristallographie*, 1966, vol. 123, pp. 1–20.

